

การสังเคราะห์สารมัธยันตร์ที่นำไปสู่ไอเซลล์ทามิเวียร์และการทำนายเชิงทฤษฎี
ของการยึดจับกับโปรตีน



นางสาวนฤวรรณ ภัทรพงศ์ดีลก

ศูนย์วิทยทรัพยากร
จุฬาลงกรณ์มหาวิทยาลัย

วิทยานิพนธ์นี้เป็นส่วนหนึ่งของการศึกษาตามหลักสูตรปริญญาวิทยาศาสตรมหาบัณฑิต

สาขาวิชาเคมี ภาควิชาเคมี


คณะวิทยาศาสตร์ จุฬาลงกรณ์มหาวิทยาลัย

ปีการศึกษา 2553

ลิขสิทธิ์ของจุฬาลงกรณ์มหาวิทยาลัย

SYNTHESIS OF INTERMEDIATES TOWARDS OSELTAMIVIR AND THEORETICAL
PREDICTION OF THEIR PROTEIN BINDING

Ms. Naruwan Pattarapongdilok



ศูนย์วิทยทรัพยากร
จุฬาลงกรณ์มหาวิทยาลัย

A Thesis Submitted in Partial Fulfillment of the Requirements
for the Degree of Master of Science Program in Chemistry

Department of Chemistry

Faculty of Science

Chulalongkorn University

Academic Year 2010

Copyright of Chulalongkorn University

Thesis Title SYNTHESIS OF INTERMEDIATES TOWARDS OSELTAMIVIR
AND THEORETICAL PREDICTION OF THEIR PROTEIN BINDING
By Ms. Naruwan Pattarapongdilok
Field of Study Chemistry
Thesis Advisor Assistant Professor Yongsak Sritana-anant, Ph.D.
Thesis Co-Advisor Assistant Professor Pornthep Sompornpisut, Ph.D.

Accepted by the Faculty of Science, Chulalongkorn University in Partial
Fulfillment of the Requirements for the Master's Degree

S. Hannongbua
..... Dean of the Faculty of Science
(Professor Supot Hannongbua, Dr.rer.nat.)

THESIS COMMITTEE

Warinthorn Chavasiri
..... Chairman
(Assistant Professor Warinthorn Chavasiri, Ph.D.)

Yks Sitt
..... Thesis Advisor
(Assistant Professor Yongsak Sritana-anant, Ph.D.)

Pd L
..... Thesis Co-Advisor
(Assistant Professor Pornthep Sompornpisut, Ph.D.)

Paitoon
..... Examiner
(Assistant Professor Paitoon Rashatasakhon, Ph.D.)

Ornjira Aruksakunwong
..... External Examiner
(Ornjira Aruksakunwong, Ph.D.)

นฤวรรณ ภัทรพงศ์ติลก : การสังเคราะห์สารมัธยันตร์ที่นำไปสู่โอเซลทามิเวียร์และการ
ทำนายเชิงทฤษฎีของการยึดจับกับโปรตีน. (SYNTHESIS OF INTERMEDIATES
TOWARDS OSELTAMIVIR AND THEORETICAL PREDICTION OF THEIR
PROTEIN BINDING) อ. ที่ปรึกษาวิทยานิพนธ์หลัก: ผศ.ดร. ยงศักดิ์ ศรีธนาอนันต์: อ. ที่
ปรึกษาวิทยานิพนธ์ร่วม: ผศ.ดร. พรเทพ สมพรพิสุทธ์, 72 หน้า

อนุพันธ์กบาาคูลินเป็นสารมัธยันตร์สำคัญในการสังเคราะห์โอเซลทามิเวียร์ฟอสเฟต หรือ
ทามิฟลู ซึ่งเป็นสารยับยั้งเอนไซม์นิวรามินิเดสของเชื้อหวัด ในงานวิจัยนี้ได้พยายามทดลอง
สังเคราะห์อนุพันธ์กบาาคูลินผ่านเบียร์ช รีดักชัน ปฏิริยาควบแน่น หรือปฏิริยาคลิสต์-แอลเคอร์
แม้ว่าปฏิริยาเบียร์ชรีดักชันจะประสบความสำเร็จในบางกรณี แต่กลับไม่ได้ผลกับการสังเคราะห์โอ
โซเมอร์ของกบาาคูลินที่ต้องการ ปฏิริยาควบแน่นของพิโรลิดีนกับไดอะซีทาลเพื่อให้ได้ไดอิน
สำหรับปฏิริยาคลิสต์-แอลเคอร์ได้เพียงผลิตภัณฑ์จากการพอลิเมอไรเซชัน ปฏิริยาไซโคลแอคดิ
ชันโดยตรงบนพิโรลได้เอซาไปไซเคิล 85 ในปริมาณน้อยเพียง 3.40 % ปฏิริยารีดักชันของสารนี้
ยังไม่สามารถให้ผลิตภัณฑ์ที่คาดไว้ การสังเคราะห์อนุพันธ์กบาาคูลินนำไปสู่การออกแบบ
โครงสร้างที่มีลักษณะคล้ายคลึงกับโอเซลทามิเวียร์ เพื่อทำนายการยึดจับกับโปรตีนของเชื้อไวรัส
ผลจากการทำนายการยึดจับของโครงสร้างที่มีลักษณะคล้ายโอเซลทามิเวียร์ทั้งหมด 34 แบบกับ
เอนไซม์นิวรามินิเดส พบว่ามีโครงสร้างของสารประกอบเพียง 2 แบบเท่านั้นที่มีพลังงานการยึดจับ
ที่เหมาะสม ผลจากการวิเคราะห์พลังงานการยึดจับและตำแหน่งของลิแกนด์แสดงให้เห็นว่า สเตอริ
โอไอโซเมอร์จะต้องมีคอนฟิกูเรชันของคาร์บอนตำแหน่งที่ 3 ต้องเป็น เอส-3-เพ็นทิล อีเทอร์ และ
สเตอริโอไอโซเมอร์ที่มีคอนฟิกูเรชันของคาร์บอนตำแหน่งที่ 4 หรือ 5 ควรเป็น อาร์-อะมิโน หรือ
อาร์-แอมโมเนียม ไอออน สำหรับโครงสร้างหลัก 1-คาร์บอกซีไซโคลเฮกซาไดอินิลของสารยับยั้ง
เอนไซม์นิวรามินิเดส

ภาควิชา.....เคมี.....ลายมือชื่อนิสิต.....นฤวรรณ ภัทรพงศ์ติลก.....
สาขาวิชา.....เคมี.....ลายมือชื่อ อ.ที่ปรึกษาวิทยานิพนธ์หลัก.....look.....
ปีการศึกษา.....2553.....ลายมือชื่อ อ.ที่ปรึกษาวิทยานิพนธ์ร่วม.....พรเทพ สมพรพิสุทธ์.....

517233323 : MAJOR CHEMISTRY

KEYWORDS: OSELTAMIVIR , TAMIFLU , GABACULINE DERIVATIVE ,
MOLECULAR DOCKING , AUTODOCK4.0

NARUWAN PATTARAPONGDILOK:SYNTHESIS OF INTERMEDIATES
TOWARDS OSELTAMIVIR AND THEORETICAL PREDICTION OF
THEIR PROTEIN BINDING. THESIS ADVISOR: ASST. PROF.
YONGSAK SRITANA-ANANT, Ph.D., THESIS CO-ADVISOR: ASST.
PROF. PORNTHAP SOMPORNPIST, Ph.D., 72 pp.

Gabaculine derivatives are the important intermediate from many reported total synthesis of oseltamivir phosphate or Tamiflu[®], the well known influenza neuraminidase inhibitor. The attempted synthesis of gabaculine derivatives were carried out via Birch reduction, condensation or Diels-Alder reaction. Although the products from some tested Birch reductions were successfully obtained, the reaction failed to give the desired gabaculine isomer. The condensation of pyrrolidine and diacetal to create the diene precursor for subsequent Diels-Alder reaction only afforded unidentifiable polymeric products. The direct cycloaddition on Boc-pyrrole gave the azabicyclic **85**, though in rather low yield of 3.40%. Subsequent reduction of this compound had not yet yielded the expected product. The synthesis of gabaculine derivatives has led to the design of 34 oseltamivir-like structures for the prediction of the viral protein binding site. The binding prediction of these potential neuraminidase inhibitors revealed that there were only two energetically favorable analogs. From analysis of relative binding energy and ligand position with respect to the reference has suggested that the suitable stereoisomers of the inhibitors in the binding sites should have (*S*)-3-pentyl ether group configuration at C3 position and either (*R*)-NH₂ or (*R*)-NH₃⁺ configurations at C4 and C5 positions respectively on the 1-carboxy-cyclohexadienyl core structure of the neuraminidase inhibitors.

Department:..... Chemistry..... Student's signature *Naruwan Pattarapongdilok*
Field of study:..... Chemistry..... Advisor's signature..... *[Signature]*
Academic year:..... 2010..... Co-Advisor's signature..... *[Signature]*

ACKNOWLEDGEMENTS

My utmost gratitude goes to my thesis advisors, Assist. Prof. Dr. Yongsak Sritana-anant and Assist. Prof. Dr. Pornthep Sompornpisut. During the time, Dr. Yongsak gave me suggestions about several things such as laboratory approach, mechanisms of reactions and the “theory of life”. Therefore, he is an important teacher in my life. Also, I acknowledge Dr. Pornthep for his kindness, knowledge about computational chemistry, and research fund.

I would like to acknowledge my thesis committee members. Assist. Prof. Dr. Warinthorn Chavasiri who was my advisor in The Inventer and Innovator Project. I still appreciate for his kind assistance and guidance, as well as his smile that made me feel happy. Assist. Prof. Dr. Paitoon Rashatasakhon’s active character is like an inspiration that gave me energy to work diligently. In addition , I humbly thank Dr. Onjira Aruksakulwong for her valuable suggestion and comments.

I would like to thank all members of Dr. Yongsak’s and Dr. Porntep’s research groups for their companionship and friendship. I also gratefully thank Mr.Arthit Vongachariya, Mr. Thanit Praneenararat, Mr. Thanet Praneenararat, Mr. Muhammad Niyomdecha, Mr. Taewarak Parnklang and Ms. Matusos Malaisree for their support and encouragement.

I would like to acknowledge the grant and funding supports provided by Center for Petroleum, Petrochemicals, and Advanced Materials.

Finally, I am forever indebted to my parents and family members for their encouragement and understanding throughout the entire study.

CONTENTS

	Page
ABSTRACT IN THAI.....	iv
ABSTRACT IN ENGLISH.....	v
ACKNOWLEDGEMENTS.....	vi
CONTENTS.....	vii
LIST OF TABLES	ix
LIST OF FIGURES	x
LIST OF SCHEMES.....	xii
LIST OF ABBREVIATIONS.....	xiii
CHAPTER I INTRODUCTION.....	1
1.1 Influenza pandemics and oseltamivir synthesis.....	1
1.2 The synthesis of interested intermediates in oseltamivir synthesis and specific synthesis.....	7
1.3 Prediction of protein binding by molecular docking.....	16
1.4 Objectives.....	17
CHAPTER II EXPERIMENT.....	19
2.1 Instrumentation.....	19
2.2 Chemicals.....	19
2.3 Synthesis of gabaculine derivatives towards oseltamivir.....	19
2.3.1 Synthesis of 3-[(<i>tert</i> -Butoxycarbonyl)amino]benzoic acid 72	19
2.3.2 Synthesis of ethyl-3-acetamidobenzoate 79	20
2.3.3 Synthesis of ethyl 3-(<i>tert</i> -butoxycarbonyl)benzoate 73	20
2.3.4 Birch reduction of 73 with Na metal.....	21
2.3.5 Birch reduction of 73 with Li metal.....	22
2.3.6 Synthesis of ethyl 3-bromopropiolate 82	22
2.3.7 Synthesis of 7-Azabicyclo[2.2.1]hepta-2,5-diene-2,7-	

	Page
dicarboxylic acid, 7-(1,1-dimethylethyl) 2-ethyl ester 85	23
2.4 Molecular docking study between proteins and ligands.....	24
2.4.1 Structure modeling of ligands.....	24
2.4.2 Structure modeling of proteins.....	27
2.4.3 Molecular docking of N1 with oseltamivir and its analogs...	27
2.4.4 Molecular docking of H5 with sialic receptor and its substrate analog inhibitors.....	29
2.4.5 Analysis of the docking results.....	30
2.4.5.1 Docking energy.....	30
2.4.5.2 RMSD.....	30
2.4.5.3 Probability score.....	30
CHAPTER III RESULTS AND DISCUSSION.....	32
3.1 Birch reduction of 3-aminobenzoic acid derivatives.....	32
3.2 Synthesis of dienamine from 2,5-dimethoxy tetrahydrofuran.....	35
3.3 Diels-Alder reaction of 1-(<i>tert</i> -butyloxycarbonyl)pyrrole.....	37
3.4 Prediction test by Autodock.....	41
3.4.1 Atomic charges and structure presentation.....	41
3.4.2 Number of trials in each Autodock run.....	43
3.5 Binding prediction of oseltamivir analogs.....	44
3.6 Binding prediction of oseltamivir analogs to hemagglutinin.....	50
CHAPTER IV CONCLUSIONS.....	51
REFERENCES.....	53
APPENDIX.....	60
VITAE.....	72

LIST OF TABLES

	Page
2.1 Substituents and stereochemical configurations on oseltamivir analogs.....	25
3.1 Protection of amine group of 96	32
3.2 Birch reduction of 73 with Na metal.....	33
3.3 Birch reduction with Li metal.....	34
3.4 The first Diels-Alder reaction pathway of 93	38
3.5 The second Diels-Alder reaction pathway of 93	39
3.6 Autodock mean energy and RMSD of the first rank (lowest E) and the most populated configurations (highest frequency) for N1-Osel docking...	42
3.7 Frequency, mean energy and RMSD from different number of trials in each Autodock run.....	43
3.8 Rank of number of run from RMSD, mean energy and %frequency.....	44
3.9 H-bond of potential compounds.....	48
A.1 Docking results of the lowest energy rank (2HU4).....	68
A.2 Docking results of the highest frequency rank (2HU4).....	69
A.3 Docking results of the lowest energy rank (1JSN).....	70
A.4 Docking results of the highest frequency rank (2HU4).....	71

LIST OF FIGURES

	Page
1.1 An influenza A virus which the three important proteins: Hemagglutinin (HA), Neuraminidase (NA) and the M2 channel.....	2
1.2 Schematic representation of an influenza virion budding from a host cell	2
1.3 Chemical structures of sialic acid receptor and influenza drugs.....	3
1.4 Chemical structure of <i>d/l</i> - gabaculine.....	7
2.1 <i>D</i> -gabaculine (m33) and <i>L</i> -gabaculine (m34).....	24
2.2 X-ray structure of oseltamivir (osel) and sialic acid (sial).....	26
2.3 Grid box in neuraminidase docking.....	28
2.4 Grid box in hemagglutinin docking.....	29
3.1 ¹ H NMR spectra of dienamine 97	36
3.2 Structure of 1-pyrrolidinepropanoic acid 81	37
3.3 ¹ H NMR spectrum of 86 in a crude mixture.....	40
3.4 $\Delta\Delta E$ obtained from the lowest energy cluster of 34 analogs.....	45
3.5 $\Delta\Delta E$ obtained from the highest frequency cluster of 34 analogs.....	45
3.6 ΔE and RMSD _{core} obtained from the lowest energy cluster of 34 analogs...	46
3.7 <i>PSE</i> vs <i>PSR</i> obtained from the lowest energy cluster of 34 analogs.....	47
3.8 Structures of m24 , m16 , m33 and m34	47
3.9 Binding of m24 and NA.....	48
3.10 The superimposition between m24 and x-ray structure of oseltamivir (pink).....	49
3.11 ΔE and RMSD _{core} obtained from the lowest energy cluster of 34 analogs	50
A.1 ¹ H-NMR (D ₂ O) Spectrum of 3-acetamidobenzoic acid 78	61
A.2 ¹ H-NMR (CDCl ₃) Spectrum of 3-[(<i>tert</i> -Butoxycarbonyl)amino]benzoic acid 72	61
A.3 ¹ H-NMR (CDCl ₃) Spectrum of ethyl-3-acetamidobenzoate 79	62
A.4 ¹ H-NMR (CDCl ₃) Spectrum of ethyl-3-(<i>tert</i> -butoxycarbonyl)benzoate 73	62
A.5 ¹ H-NMR (CDCl ₃) Spectrum of <i>tert</i> -Butyl[3-(hydroxymethyl)phenyl] carbamate 89 in a mixture.....	63

	Page
A.6 ¹ H-NMR (CDCl ₃) Spectrum of <i>N</i> -(<i>tert</i> -butoxycarbonyl)- <i>m</i> -toluidine 90 in a mixture.....	63
A.7 ¹ H-NMR (CDCl ₃) Spectrum of <i>tert</i> -butyl cyclohexa-2,5-dienylcarbamate 80	64
A.8 ¹ H-NMR (CDCl ₃) Spectrum of ethyl-2-(<i>N</i> -pyrrolidinye)propanoate 81	64
A.9 ¹ H-NMR (CDCl ₃) Spectrum of ethyl 3-bromopropiolate 82	65
A.10 ¹ H-NMR (CDCl ₃) Spectrum of ethyl-2-(<i>N</i> - <i>tert</i> -butoxycarbonyl)pyrrolyl propanoate 83	65
A.11 ¹ H-NMR (CDCl ₃) Spectrum of 7-Azabicyclo[2.2.1]hepta-2,5-diene-2,7- dicarboxylic acid, 7-(1,1-dimethylethyl) 2-ethyl ester 85	66
A.12 ¹ H-NMR (CDCl ₃) Spectrum of 7-Azabicyclo[2.2.1]hept-5-ene-2,7- dicarboxylic acid, 7-(1,1-dimethylethyl) 2-ethyl ester 86	66
A.13 ¹ H-NMR (CDCl ₃) Spectrum of 1,4(<i>N</i> -morpholinyl)-butadiene 97	67

LIST OF SCHEMES

	Page
1.1 The preparation of epoxide intermediate 12 from quinic acid 7	4
1.2 The synthesis of oseltamivir phosphate from the epoxide 12	5
1.3 The preparation of epoxide intermediate for synthesis of Tamiflu®	6
1.4 Synthesis of Tamiflu®.....	6
1.5 Corey's synthesis of oseltamivir.....	8
1.5 Kann's synthesis of oseltamivir.....	9
1.7 Okamura's synthesis.....	10
1.8 Trost's synthesis of oseltamivir.....	11
1.9 Sharpless' synthesis of gabaculine.....	12
1.10 Danishefsky's synthesis of isogabaculine.....	13
1.11 Trost's synthesis of gabaculine.....	13
1.12 Birch's synthesis of gabaculine.....	14
1.13 Frater's synthesis.....	15
1.14 Hiemstra's synthesis of gabaculine.....	15
1.15 Gabaculine derivatives synthesis via Birch Reduction.....	17
1.16 Gabaculine derivatives synthesis via condensation and Diels-Alder reaction.....	17
1.17 Gabaculine derivatives synthesis via by Diels-Alder and reduction reaction.....	18
1.18 Strategies of <i>in-silico</i> for prediction of protein-ligand binding.....	18
3.1 Dioxime from trapped succinic dialdehyde.....	35
3.2 The condensation reaction of 76 and secondary amine.....	35
3.3 The condensation reaction of hydrolyzed 76	35
3.4 Synthesis of gabaculine via Diels-Alder and reduction reactions.....	37
3.5 The reduction of 85 with NaBH ₄	39
3.6 The terminal bromination of ethyl propiolate 94	40
3.7 The Diels-Alder reaction of 93 and 82	40
4.1 Birch reduction of protected amonobenzoate 73	51
4.2 A side reaction during a condensation attempt.....	51
4.3 The direct cycloaddition of 93	52

LIST OF ABBREVIATIONS

°C	: degree celsius
μ	: micro
¹ H-NMR	: proton nuclear magnetic resonance spectroscopy
Ac ₂ O	: acetic anhydride
AcCl	: acetyl chloride
AcOH	: acetic acid
AlCl ₃	: aluminium chloride
ARG	: arginine
ASP	: aspartic acid
bd	: broad doublet
(Boc) ₂ O	: <i>tert</i> -butyl pyrocarbonate
bs	: broad singlet
CDCl ₃	: deuterated chloroform
CH ₂ Cl ₂	: dichloromethane
d	: doublet
D ₂ O	: deuterated water
dd	: doublet of doublet
DMF	: <i>N, N</i> -dimethylformamide
DMSO	: dimethyl sulfoxide
Et ₂ O	: diethyl ether
Et ₃ SiH	: triethylsilane
EtOAc	: ethyl acetate
EtOH	: ethanol
GLU	: glutamine acid
HA	: hemagglutinin
Hz	: Hertz
IC ₅₀	: inhibitory concentration
<i>J</i>	: coupling constant
kcal	: kilocalories
m	: multiplet

MeOH	: methanol
min	: minute
mL	: milliliter
MsCl	: methanesulfonyl chloride
NA	: neuraminidase
NaBH ₄	: sodium borohydride
NaHCO ₃	: sodium hydrogen carbonate
NBA	: <i>N</i> -bromoacetamide
NH ₄ Cl	: ammonium chloride
NMR	: nuclear magnetic resonance spectroscopy
Ph ₃ P	: triphenyl phosphine
ppm	: parts per million (unit of chemical shift)
py.	: pyridine
q	: quartet
RMSD	: root mean square deviation
s	: singlet
SOCl ₂	: thionyl chloride
t	: triplet
<i>t</i> -BuOH	: <i>tert</i> -butanol
TFA	: trifluoroacetic acid
THF	: tetrahydrofuran
TLC	: thin layer chromatography
TMSCl	: trimethylsilyl chloride
TMSCN	: trimethylsilyl cyanide
TYR	: tyrosine
δ	: chemical shift

CHAPTER I

INTRODUCTION

1.1 Influenza pandemics and oseltamivir synthesis

The potential for an influenza pandemic is a worldwide concern. The very first pandemic of influenza was known as the Spanish flu (1918, H1N1 strain). The subtype killed 20-40 million people worldwide [1]. The Asian flu (1957, H2N2, 1-2 million casualties) originated from poultry infection in Hong Kong killed humans with lethality rate over 50% [2, 3, 4]. It is estimated that if a similar event took place today, about 30% of the world's population could die. Recently, the 2009 flu pandemic caused by new strain of H1N1 virus was the result of the previous triple reassortment among avian, swine and human flu viruses [5]. The outbreak was reported to originate from North America and still continued to spread globally until now [6].

The influenza viruses were roughly classified into types A, B, and C. The type A virus is characterized based on the structure of the two surface proteins: Hemagglutinin (HA) and Neuraminidase (NA). HA is known to mediate the binding of viruses to target cells via their terminal sialic acid (1) receptor of the cell membrane and NA catalyzes the removal of these terminal sialic acid linked to glycoproteins and glycolipids of the infected host cells [7-10]. The influenza A virus also contains a proton channel M2 protein which is not present in type B and C viruses (**Figure 1.1** and **Figure 1.2**) [9].

ศูนย์วิทยทรัพยากร
จุฬาลงกรณ์มหาวิทยาลัย

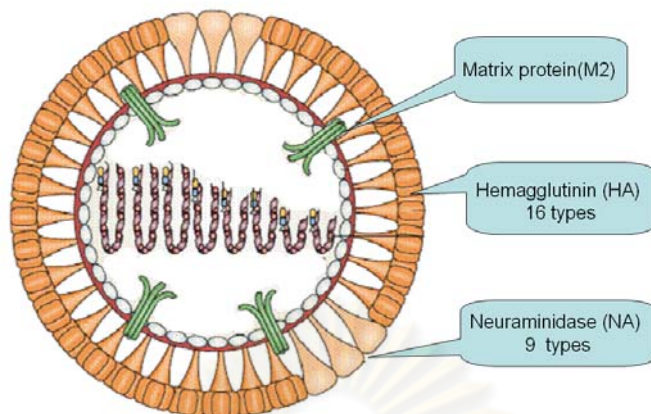


Figure 1.1 An influenza A virus which the three important proteins: Hemagglutinin (HA), Neuraminidase (NA) and the M2 channel [11]

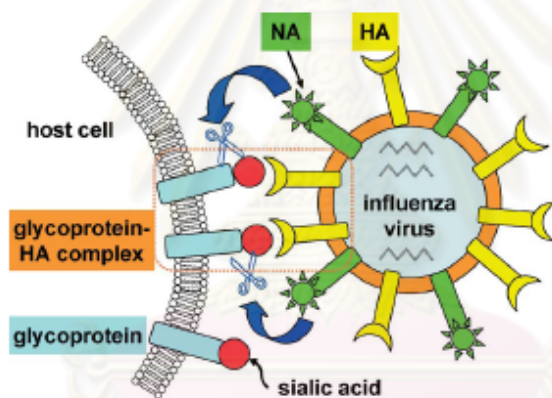


Figure 1.2 Schematic representation of an influenza virion budding from a host cell [12]

ศูนย์วิทยทรัพยากร
จุฬาลงกรณ์มหาวิทยาลัย

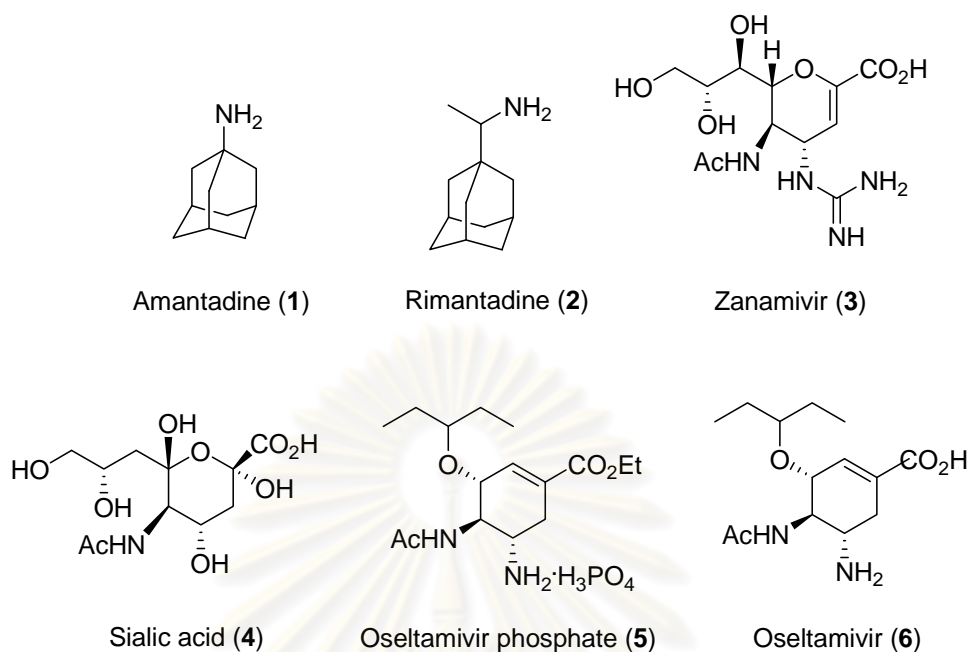


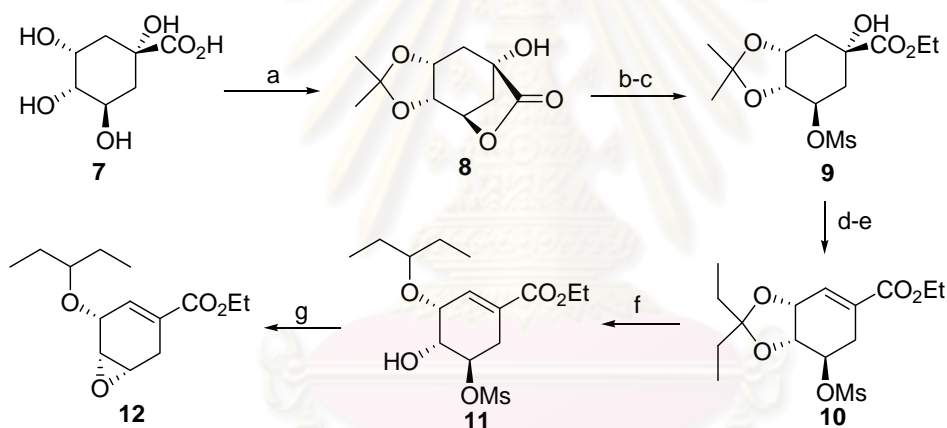
Figure 1.3 Chemical structures of sialic acid receptor and influenza drugs

The drugs amantadine and rimantadine can both help prevent and relieve the symptoms of influenza A infections in adults. Inhibitors of the M2 proton pump use of amantadine **1** and rimantadine **2**, clinically effective inhibitors has been thwarted by the emergence of drug resistance and by toxic side effect. In addition, there is a serious limitation that they could be applicable to influenza A only [13]. In contrast, NA catalyzes the cleavage of sialic acid residues **4** from glycoproteins and liberates the budding virion from host cell, inhibiting entrapment and self-aggregation. So neuraminidase is a potential enzyme for viral replication and there are in all there classes of influenza virus [14, 15]. Two anti-influenza drugs, zanamivir (**3**: GlaxoSmithKleins, Relenza) [16] and oseltamivir phosphate (**5**: Gilead's Tamiflu, marketed by Roche) [9, 10] have reached the market in July and October 1999 respectively.

Zanamivir and oseltamivir phosphate can strongly bind to the active site of NA with the IC₅₀ values in the nanomolar range. Zanamivir has low bioavailability and is administered by inhalation, which can cause problems in respiratory disease patients [10]. While oseltamivir phosphate which is an orally active prodrug of the corresponding active carboxylic acid form **6**, can be conveniently administered as capsules and has higher bioavailability than zanamivir [10]. This has led to global demand for stockpiles of

oseltamivir. Due to its significance but potentially limited production, alternative routes besides the current industrial synthesis of oseltamivir have become an intensive research.

Oseltamivir was discovered in 1997 by Gilead and coworker, in which its synthetic process has been further developed by Roche into industrial production route to oseltamivir phosphate or Tamiflu[®] **5** [17-25]. The synthesis started from (-)-quinic acid **7** that was converted to the acetonide with concomitant lactonization to give **8** (**Scheme 1.1**). The lactone was re-opened with sodium ethoxide in ethanol followed by mesylation to produce the ethyl ester **9**. The ester **9** was dehydrated with sulfuryl chloride and transketalized with 3-pentanone in the presence of catalytic perchloric acid to give **10**. Trimethylsilyltriflate and borane dimethyl sulfide complex were used to reduce the 3,4-pentylidene ketal to give **11**. The product **11** was treated with potassium bicarbonate in aqueous ethanol to generate epoxide **12** in 60% yields from **7**.

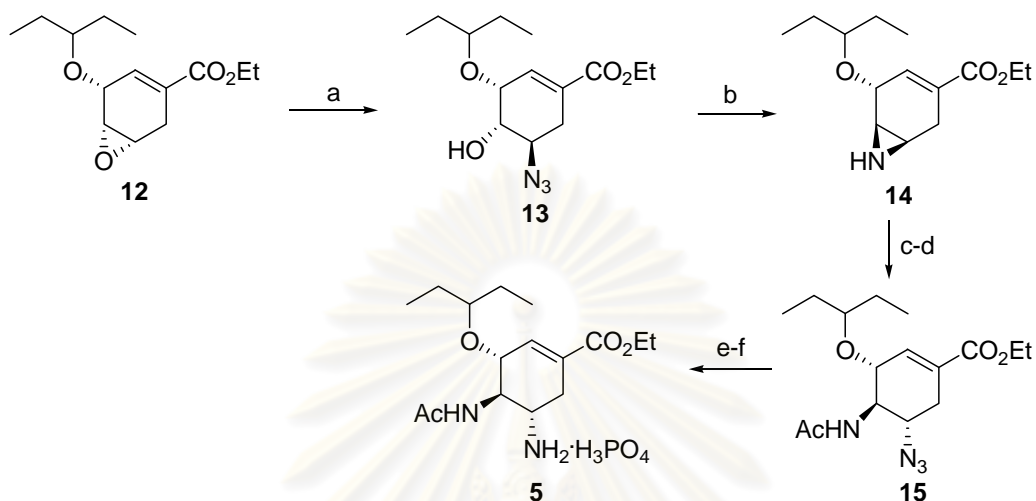


(a) acetone dowex resin, PhH, DMF, reflux, 79%, (b) NaOEt, EtOH, 96%, (c) MsCl, DMAP, py, 92%, (d) SOCl₂, py, CH₂Cl₂, -20°C to -30°C, (e) 3-pentanone, cat.HClO₄, 95%, (f) TMSOTf, BH₃-SMe₂, CH₂Cl₂, -20°C, 75%, (g) KHCO₃, aq.EtOH, 1h, 96%.

Scheme 1.1 The preparation of epoxide intermediate **12** from quinic acid **7**

The continued synthesis from the intermediate **12** has become the first large scale synthesis of oseltamivir (**Scheme 1.2**). Epoxide **12** was heated with sodium azide and ammonium chloride in aq. ethanol to give azido – alcohol **13**, which was subjected to reductive cyclization with trimethyl phosphine to afford aziridine **14**. Ring opening of the aziridine **14** with sodium azide in the presence of ammonium chloride gave an azidoamine, which was directly acetylated with acetic anhydride to generate azidoacetamide **15** in 37% yield from epoxide **12**. Azide **15** was reduced with Raney

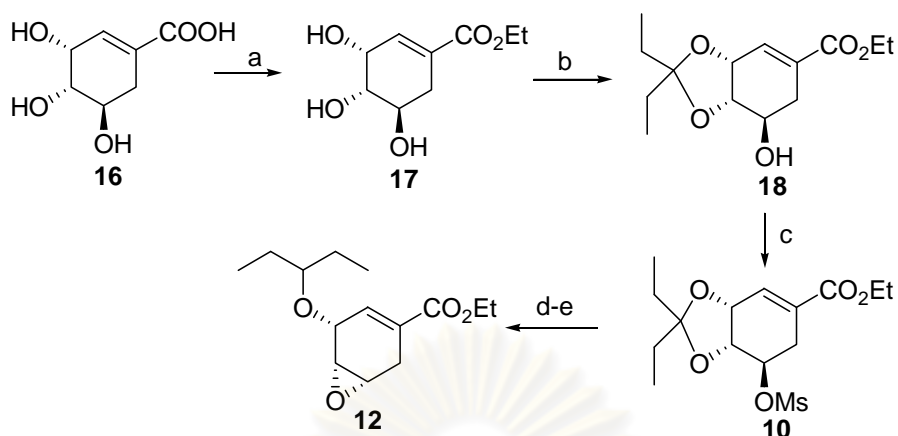
nickel in ethanol and followed by salt formation with phosphoric acid to afford the oseltamivir phosphate **5**.



(a) NaN_3 , NH_4Cl , EtOH , H_2O , $70-75^\circ\text{C}$, 12-18h, 86%, (b) Me_3P , MeCN , 35°C , 97%, (c) NaN_3 , NH_4Cl , DMF , $70-80^\circ\text{C}$, 12-18h, 44%, (d) Ac_2O , NaHCO_3 , hexane, CH_2Cl_2 , 1h, 44% 2 steps, (e) Ra-Ni , EtOH , 35°C , 10-16h, (f) H_3PO_4 , EtOH , $55-65^\circ\text{C}$ to rt 3-24h, 71%, 2 steps.

Scheme 1.2 The synthesis of oseltamivir phosphate from the epoxide **12**

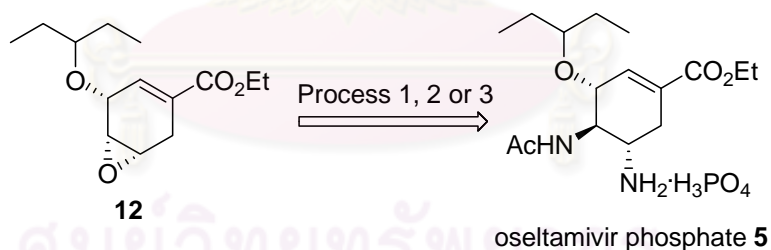
Federspiel and coworkers [19] developed and optimized the oseltamivir synthesis starting from (-)-shikimic acid **16**, either extracted from Chinese star anise or ginkgo leaves or from fermentation using a genetically engineered *E. coli* strain (**Scheme 1.3**). (-)-Shikimic acid **16** was refluxed with SOCl_2 in EtOH to give ethyl shikimate **17** and treated with 3-pentanone in the presence of TfOH to afford pentylidene ketal **18**. The intermediate **10** was generated from mesylation of the remaining hydroxyl group with mesyl chloride and Et_3N . Ring opening with triethyl silane and TiCl_4 at -32° to -36°C followed by basic treatment with NaHCO_3 in EtOH to give epoxide intermediate **12** in 64% yields from **16**.



(a) SOCl_2 , EtOH, reflux, 97%, (b) 3-pentanone, TfOH, 98%, (c) MsCl, Et_3N , EtOAc, 89%,
 (d) Et_3SiH , CH_2Cl_2 , -32 to -36°C , 87%, (e) NaHCO_3 , aq.EtOH, 96%.

Scheme 1.3 The preparation of epoxide intermediate for synthesis of Tamiflu[®]

Roche and coworker developed three processes by the synthesis of **5** from epoxide **12**. The first azide-free synthesis was reported by Karpf *et al.* (2001) [22]. Currently, the industrial production uses this route because the economical of this synthesis while the allylamine and the tert-butylamine routes were later reported as the alternative direction using hazardous azide reagents (**Scheme 1.4**) [18-25].



- 1: azide route, 5 steps, 50-55%
- 2: allylamine route, 8 steps, 35-40%
- 3: tert-butylamine route, 6 steps, 60%

Scheme 1.4 Synthesis of Tamiflu[®]

1.2 The synthesis of interested intermediates in oseltamivir synthesis and specific synthesis

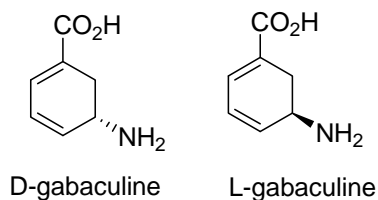
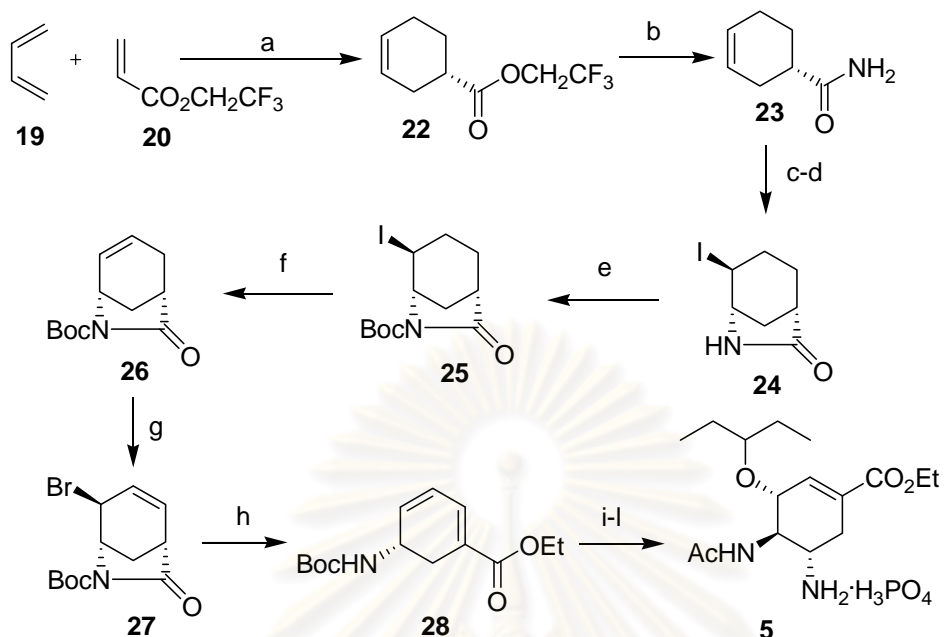
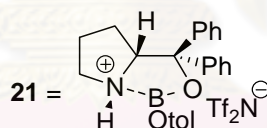


Figure 1.4 Chemical structure of *d/l*- gabaculine

Among many synthetic strategies, gabaculine derivatives are one of the most encountered intermediates reported in many recent total synthesis of oseltamivir. In 2006, Corey and coworkers [26] reported a concise azide-free synthesis of **5** starting from the Diels-Alder reaction between butadiene and trifluoroethyl acrylate in the presence of the proline-derived catalyst (**Scheme 1.5**). Ammonolysis of the adduct **22** produced amide **23** quantitatively. Iodolactamization of **23** using the Knapp protocol [28] generated lactam **24**, which was protected and removed the iodide group with diazobicycloundecene (DBU) to give **26**. Compound **27** was then efficiently generated by allylic bromination. Treatment of **27** with cesium carbonate in ethanol afforded the gabaculine derivative **28**.

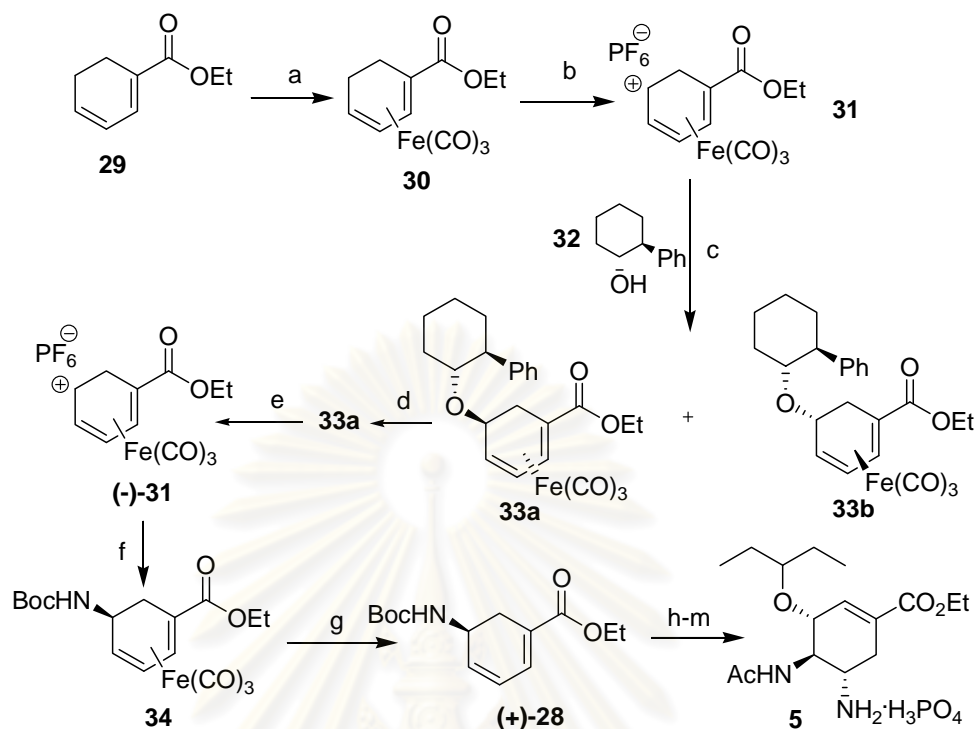


(a) **21** 10 mol% neat, 23°C, 30h, 97%, (b) NH₃, CF₃CH₂OH, 40°C, 5h, 100%, (c) TMSOTf, Et₃N, pentane, (d) I₂, Et₂O/THF, 2h, (e) (Boc)₂O, Et₃N, DMAP, CH₂Cl₂, 4h, 99%, (f) DBU, THF, reflux, 12h, 96%, (g) NBS, cat. AIBN, CCl₄, reflux, 2h, 95%, (h) Cs₂CO₃, EtOH, 25 min, 100%, (i-l) Ref.[27].



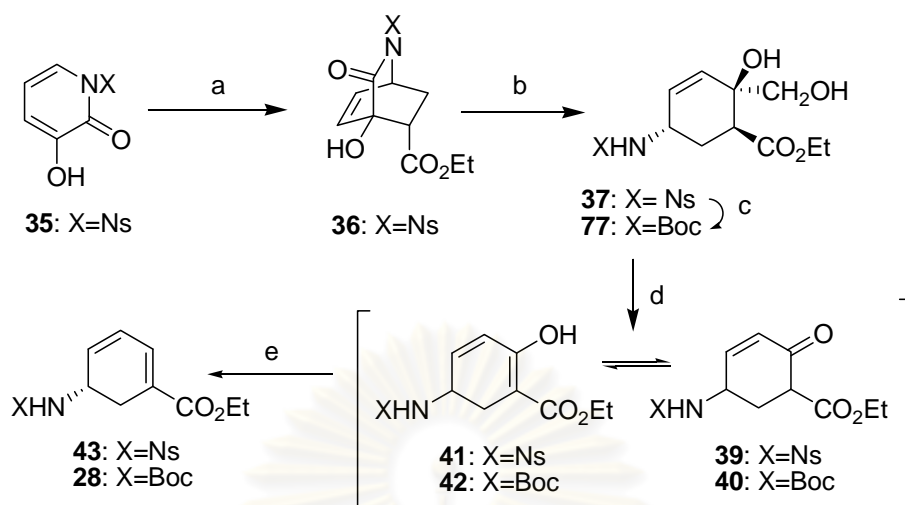
Scheme 1.5 Corey's synthesis of oseltamivir

Kann and coworkers [29] utilized stereoselective amination of cationic iron carbonyl complex as the key step of oseltamivir synthesis (Scheme 1.6). The synthesis started with a tandem Michael/Wittig reaction between (*E*)-ethyl-4-bromobut-2-enoate and acrolein to generate cyclohexadiene **29**. Then it was treated with diiron nanocarbonyl to provide racemic complex **30**. This complex underwent hydrogen abstraction with Ph₃CPF₆ to produce salt **31**, which was then trapped with chiral alcohol **32** to afford a diastereomeric mixture which was separated by preparative HPLC to give the desired diastereomer **33a** (47% yield). Enantiomerically (-)-**31** was obtained by treatment with HPF₆. Trapping with BocNH₂ and a subsequent oxidative decomplexation with H₂O₂ afforded the gabaculine intermediate **28**. (+)-**28**.



Scheme 1.6 Kann's synthesis of oseltamivir

Recently, Okamura and coworkers [30] published a short synthesis of racemic Corey's gabaculine intermediate as shown in **Scheme 1.7**. The bicyclic lactam **36** adduct was obtained by base-catalyzed Diels-Alder reaction of *N*-nosyl-3-hydroxy-2-pyridone **35** with ethyl acrylate. The gabaculine intermediate was obtained in 45% overall yield in four steps from the adduct **36**. These steps included the reductive cleavage of lactam ring, the oxidative cleavage of vicinol diol, the carbonyl reduction and finally the elimination of the resulted hydroxyl group. The yield of the Nosyl-protected gabaculine **43** was 33% starting from **37** which the Boc-protected on **28** was 61% starting from **77**.

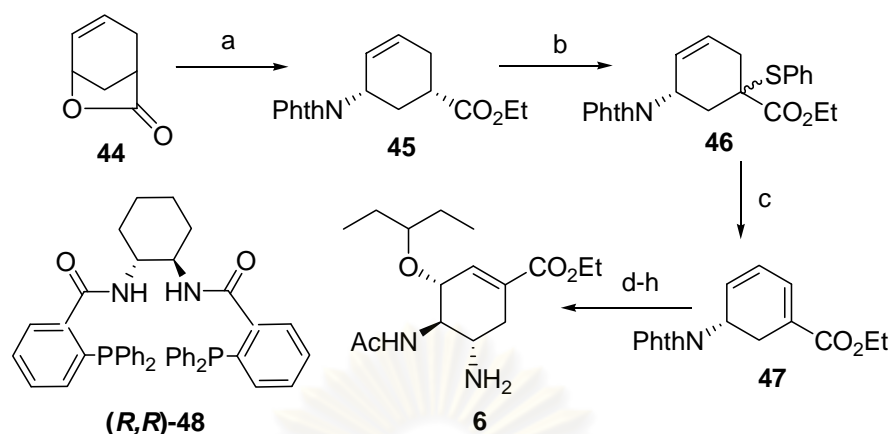


(a) aq NaOH, ethyl acrylate, 83%, (b) NaBH₄, THF, 77%, (c) PhSH, K₂CO₃, CH₃CN, 55%, (d) BaIO₄, aq THF, (e) i) NaBH₄, EtOH, ii) MsCl, Et₃N, DMAP, CH₂Cl₂ (61% from **77**, 33% from **37**)

Scheme 1.7 Okamura's synthesis

Trost *et al.* [31] opened the racemic lactone **44** and desymmetrized with the use of $[(\eta^3\text{-C}_3\text{H}_5\text{PdCl})_2]$ and the ligand (*R,R*)-**48** as the catalyst with phthalimide as the nucleophile (**Scheme 1.8**). Subsequence esterification and sulfenylation with PhSSO₂Ph and KHMDS gave the α -thioester **46**. Oxidation of this diastereomeric mixture with mCPBA followed by thermal elimination *in situ* gave the gabaculine intermediates **47** and 5 steps generated to oseltamivir.

ศูนย์วิทยทรัพยากร
จุฬาลงกรณ์มหาวิทยาลัย

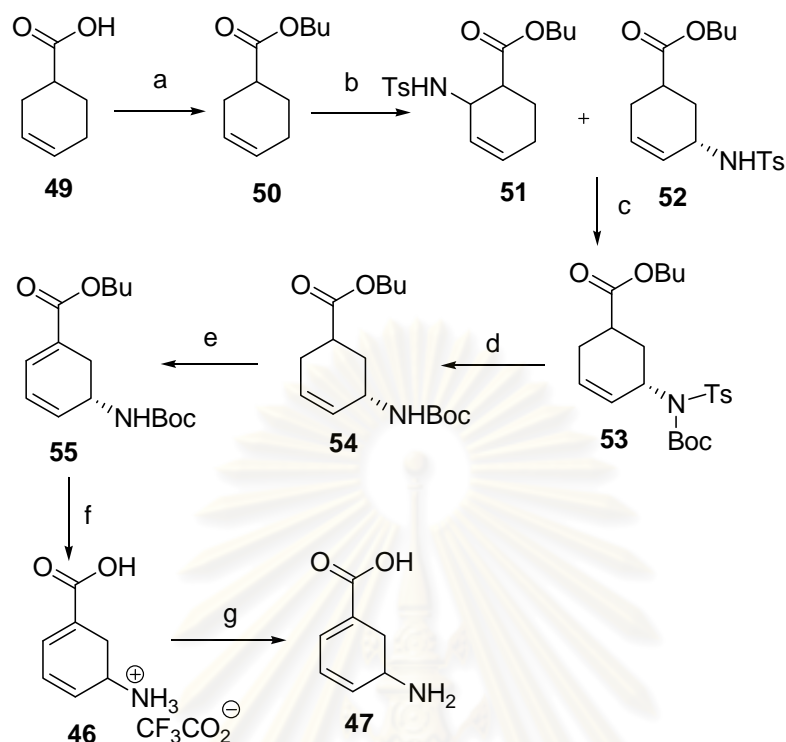


(a) 2.5 mol%[(η^3 -C₃H₅PdCl)₂], 7.5 mol% (*R,R*)-13, 1.5 eq trimethylsilylphthalimide, THF, 40%, then TsOH·H₂O, EtOH, reflux, 84%, 98%ee,
 (b) 1.5 eq KHMDS, 1.8 eq PhSSO₂Ph, THF, -78°C to rt, 94%, (c) 1 eq *m*CPBA, 2 eq NaHCO₃, 0°C, then 1eq DBU, 60°C, toluene, 85%
 (d-h) Ref [31].

Scheme 1.8 Trost's synthesis of oseltamivir

In fact, gabaculine itself has been the target of many syntheses in earlier attempts that may not related to oseltamivir. Sharpless *et al.* [32] synthesized *dl*-gabaculine utilizing direct allylic amination as the key step (**Scheme 1.9**). This target was obtained in 7 steps from 3-cyclohexene-1-carboxylic acid as the starting material in 23% overall yield.

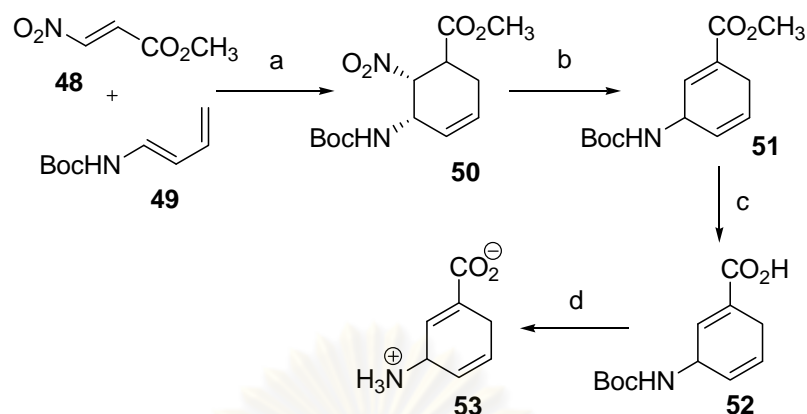
ศูนย์วิทยทรัพยากร
 จุฬาลงกรณ์มหาวิทยาลัย



(a) Isobutylene, H_2SO_4 , ether, 25°C , 79%, (b) i) 1.2 eq of $\text{TsN}=\text{S}=\text{NTs}$, CH_2Cl_2 , 25°C , ii) K_2CO_3 in 60% $\text{CH}_3\text{OH}-\text{H}_2\text{O}$, (70% 4:5=1:3 mixture of isomer), (c) i) NaH , DMF, 25°C , ii) *tert*-Boc azide, (d) electrolysis (-2.1V) in 0.2 M TEAB in MeCN, 92%, (e) i) 3.6 eq of lithium cyclohexylisopropylamide, THF, -78°C , ii) I_2 , THF, -78°C , iii) DABCO, benzene, 25°C , (90% overall from 12), (f) CF_3COOH , (g) ion-retarding resin

Scheme 1.9 Sharpless' synthesis of gabaculine

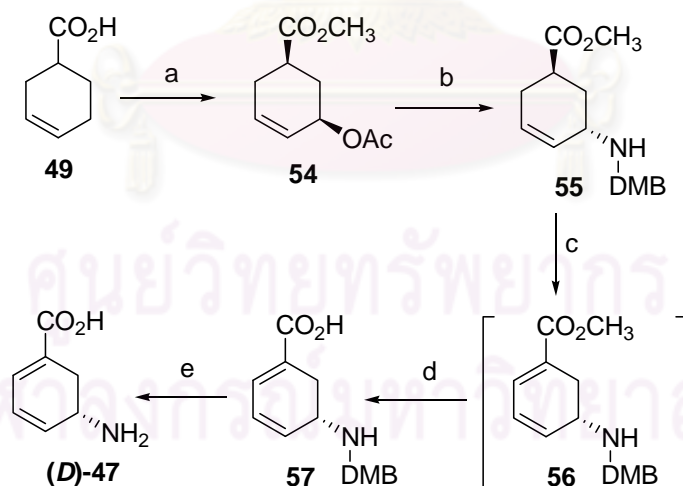
Danishefsky and coworkers [33] reacted 1-(*N*-acylamino)-1,3-diene **48** with nitro acrylate to give the Diels-Alder adduct **50** (Scheme 1.10). The dihydrobenzene derivative **51** was generated from treatment of **50** with diazobicycloundecene (DBU) in 70% yield. Finally, hydrolysis of the ester group with aqueous NaOH followed by deprotection and immediate extraction gave the regioisomer of gabaculine **52** in 73% yields.



(a) benzene, rt, 3h, 68%, (b) 1eq DBU, THF, 5°C, then rt, 6h (c) aq NaOH, 55°C, 6h, then conc.HCl, (d) i) 0.1 N HCl, 55°C, 24h, ii) Bio-Rod AG 11A8 ion retardation resin.

Scheme 1.10 Danishefsky's synthesis of isogabaculine

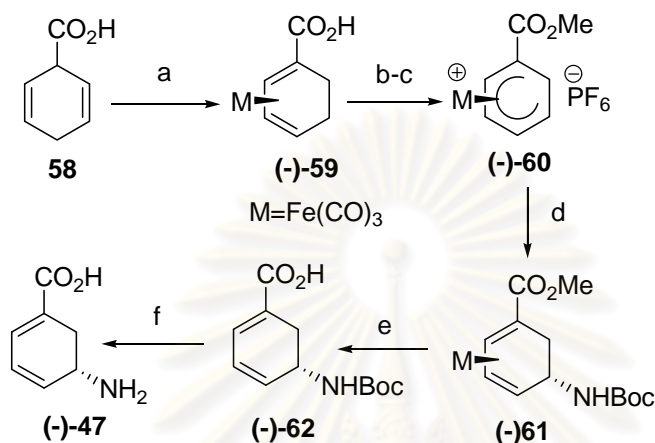
Trost and coworkers [34] used their approach towards primary allylic amines via transition-metal-catalyzed reactions to give (\pm)-gabaculine (**Scheme 1.11**). This regiocontrolled synthesis of (\pm)-gabaculine which was obtained in 45% overall yield from 3-cyclohexenecarboxylic acid **49**, was reported to selectively react at the less substituted end of the allyl unit regardless of the regioisomer of the starting material.



(a) Ref.[34] , (b) tetrakis(triphenylphosphine)palladium, DMBNH₂, rt ,81%, (c) i) LDA, THF, -78°C and then I₂, ii) DABCO, (d) 2% NaOH, H₂O, 1,4-dioxane, (e) 88% HCO₂H, 60°C.

Scheme 1.11 Trost's synthesis of gabaculine

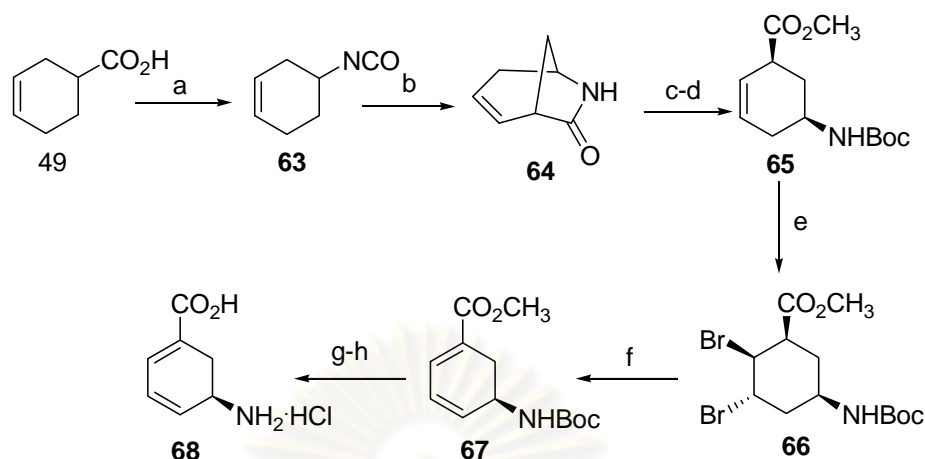
Birch *et al.* [35] performed a lateral control of structure and reactivity exemplified by enantiospecific synthesis of (+)-gabaculine or (-)-gabaculine (**Scheme 1.12**). They report this synthesis using tricarbonyl iron complex of gabaculine, the control features and capabilities of complexes of metal atoms were resolved.



(a) Ref.[35] , (b) CH_2N_2 , Et_2O , (c) $\text{Ph}_3\text{C}^+\text{PF}_6^-$, CH_2Cl_2 , (d) Me_3NO , $\text{CH}_3\text{CONMe}_2$, -15°C , 3h, then 0°C , 16h, (e) NaOH , MeOH , H_2O , (f) 3M HCl , MeOH , ion-exchange, H_2O .

Scheme 1.12 Birch's synthesis of gabaculine

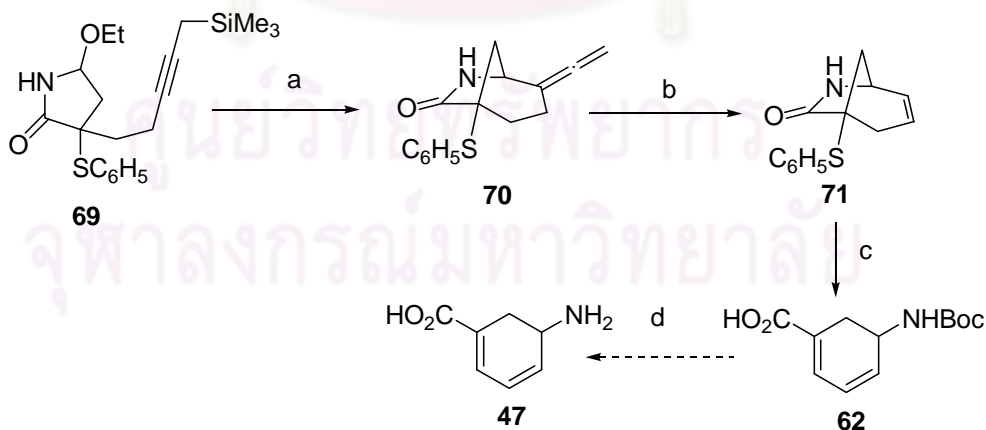
Frater *et al.* [36] converted 3-cyclohexen-1-carboxylic acid **49** to **63** carrying the isocyanate group (**Scheme 1.13**). Cyclization of **63** was carried out in PPA to give **64** which was reopened with SOCl_2 in methanol and di-*t*-butyl-carbonate to give the protected amino acid **65**. Then bromination of **65** and double eliminations provided the protected gabaculine **67**. Finally, gabaculine hydrochloride **68** was generated by removing the protecting groups and recrystallization.



(a) ClCO_2Et , Et_3N , NaN_3 , 79%, (b) PPA, 50%, (c) SOCl_2 , MeOH, 85% (d) Boc_2O , Et_3N , (e) Br_2 , CCl_4 , 90%, (f) LiBr , LiCO_3 , HMPTA 20°C, 5 h, then 40°C, 3.5 h, (g) 2% NaOH in dioxane, 89%, (h) HOAC, sat. with HCl , 72%.

Scheme 1.13 Frater's synthesis

Hiemstra and coworkers [37] synthesized (\pm)-gabaculine using dipolar bifunctional reagent (Scheme 1.14). The propargylic silane **69** was cyclized into the bicyclic lactam **70**, which was subjected to ozonolysis of the allene moiety and subsequent Shapiro reaction to give **71**. The lactam was then hydrolyzed using Grieco's method [38] followed by sulfur oxidation and sulfoxide elimination to give *N*-(tert-butoxycarbonyl) – gabaculine **62**.



(a) HCO_2H , 87%, (b) i) O_3 , then Me_2S , ii) TsNHNH_2 , iii) $n\text{-BuLi}$, 56%, (c) i) (Boc_2O), Et_3N , DMAP, ii) MCPBA, iii) LiOH , H_2O , THF, (d) Ref.[37].

Scheme 1.14 Hiemstra's synthesis of gabaculine

1.3 Prediction of protein binding by molecular docking

Automated docking is widely used for predicting of biomolecular binding phenomena in structure/function analysis and in molecular design. AutoDock is one of molecular docking programs that has proven to be an effective tool capable of quickly and accurately predicting bound conformations and binding energies of ligands with macromolecular targets. The program used a semiempirical free energy force field to predict binding free energies of small molecules to their macromolecular receptors [39]. There appeared many recent researches using AutoDock concerning the study of combating Influenza. For example, Cheng *et al.* [40] used AutoDock 4.0 to screen the NCIDS (National Cancer Institute (NCI) diversity set) against representative receptor ensembles extracted from explicitly solvated molecular dynamics simulations of the neuraminidase system, which revealed potential novel antiviral compounds for avian influenza neuraminidase.

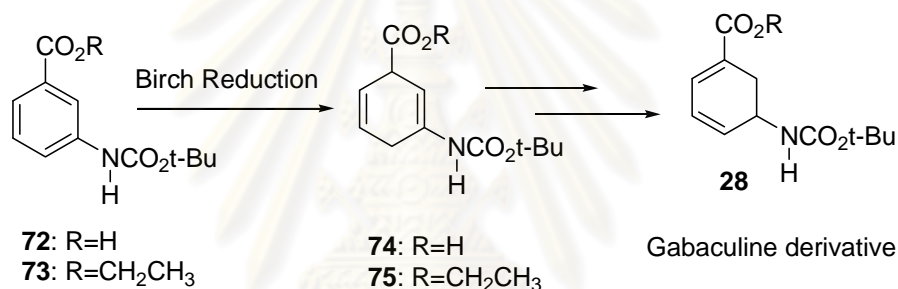
In another study, Glide XP version 4.5 and AutoDock version 4.0 were used to screen a set of 65,000 compounds from the ZINC database. All the AutoDock calculations were carried out with the Chemomomentum system. Combining the AutoDock and Glidescore values generated a consensus score derived from the arithmetical average of both scores. The result shown that the binding sites of wild-type avian influenza A H5N1 neuraminidase were adjacent to the binding sites of the open conformation of the virus protein, as well as those of the Tamiflu[®]-resistant H274Y variant. The compounds with the best computed free energies of binding, in agreement by two docking methods, consensus scoring, and ligand efficiency values, suggested that mimicking a polysaccharide, β -lactam, and other structures, including some known drugs, could be the potential routes for multi binding site of the inhibitor design [41].

Kalliokoski and coworkers [42] used AutoDock to perform a retrospective virtual screening on 19 drug targets with a publicly available data set. They proposed that tautomer and protomer prediction could significantly save computing resources and yield similar results to enumeration.

In addition, Durrant *et al.* [43] studied the potential drug-like inhibitors of group 1 influenza neuraminidase identified through computer-aided drug design. They used the computer program Auto-Grow and AutoDock to generate novel predicted neuraminidase inhibitors. Auto-Grow gave great flexibility of the neuraminidase active site, also incorporated protein dynamics into the computer-aided drug-design process. Several potential inhibitors were identified with predicted neuraminidase binding better than currently some approved drugs.

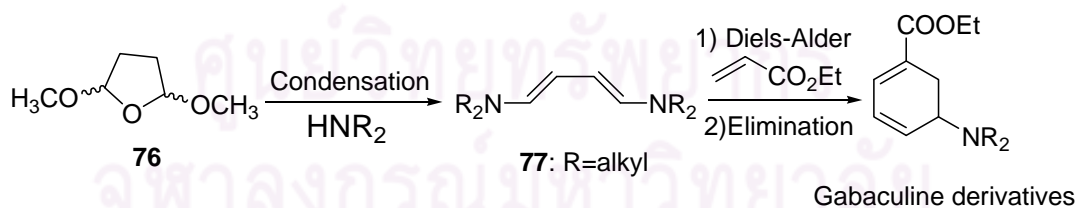
1.4 Objectives

1.4.1 Synthesis of gabaculine derivatives from 3-aminobenzoic acid by Birch reduction



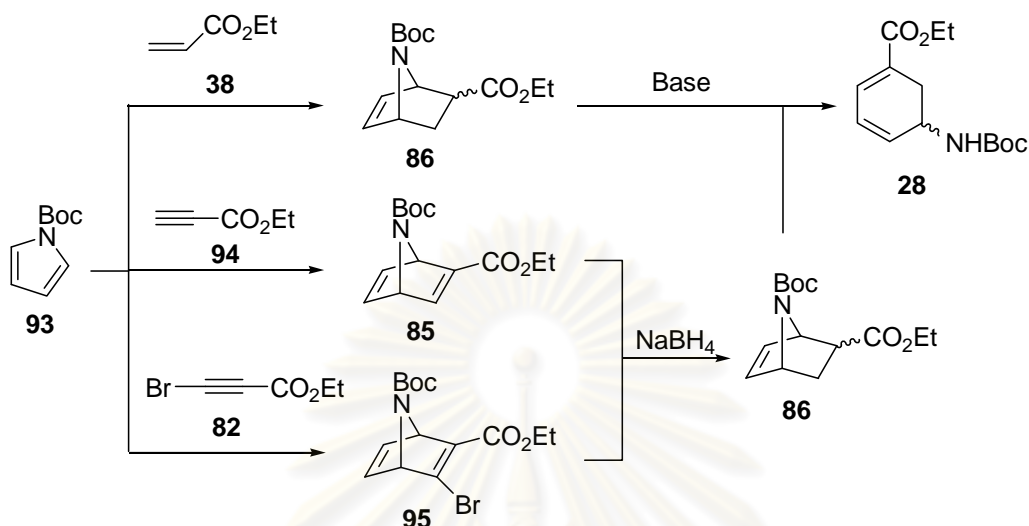
Scheme 1.15 Gabaculine derivatives synthesis via Birch Reduction

1.4.2 Synthesis of gabaculine derivatives from 2,5-dimethoxy tetrahydrofuran by condensation reaction, Diels-Alder and elimination



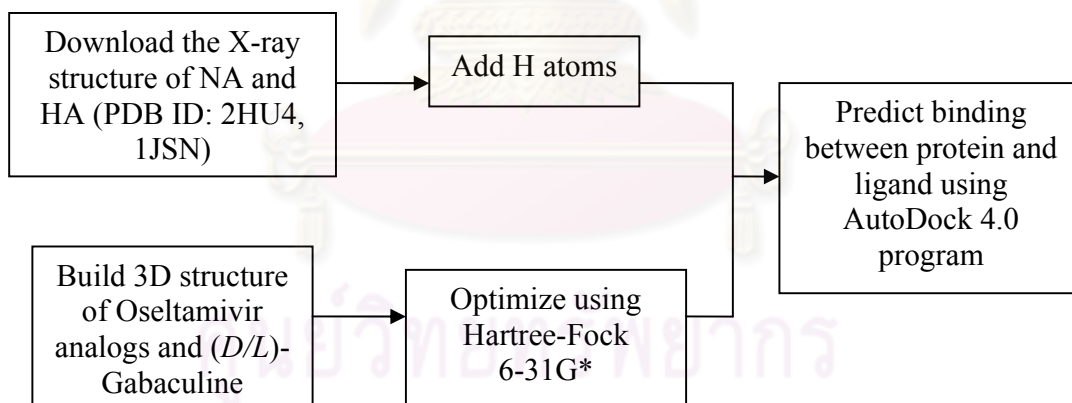
Scheme 1.16 Gabaculine derivatives synthesis via condensation and Diels-Alder reaction

1.4.3 Synthesis of gabaculine derivatives by Diels-Alder, reduction and ring – opening reaction



Scheme 1.17 Gabaculine derivatives synthesis via by Diels-Alder and reduction reaction

1.4.4. Prediction of Neuraminidase and Hemagglutinin binding with *in-silico* designed by Molecular docking method



Scheme 1.18 Strategies of *in-silico* for prediction of protein-ligand binding

CHAPTER II

EXPERIMENT

2.1 Instrumentation

The following analytical methods were used throughout this work unless otherwise indicated.

The $^1\text{H-NMR}$ spectra were obtained in either CDCl_3 , DMSO-d_6 or D_2O solution using Varian Mercury NMR spectrometer, which operated at 400.00 MHz for ^1H nuclei (Varian Company, CA, USA).

2.2 Chemicals

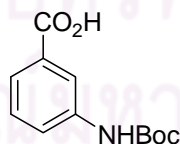
Thin layer chromatography (TLC) was performed on aluminium sheets precoated with silica gel (Merck Kieselgel 60 F254) (Merck KgaA, Darmstadt, Germany).

Column chromatography was performed using silica gel (0.06-0.2 mm or 70-230 mesh ASTM), Merck Kieselgel 60 G (Merck KgaA, Darmstadt, Germany). Solvents used as the mobile phase for column chromatography were distilled from commercial-grade solvents.

Chemicals and solvents were used as purchased unless otherwise noted.

2.3 Synthesis of gabaculine derivatives towards oseltamivir

2.3.1 Synthesis of 3-[(*tert*-Butoxycarbonyl)amino]benzoic acid **72** [27]

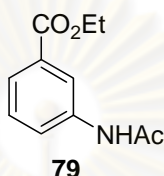


72

A solution of NaHCO_3 (0.806 g, 9.60 mmol) in water (15 mL) was added 3-aminobenzoic acid (0.6581 g, 4.80 mmol). Boc_2O (1.2635 g, 5.79 mmol) in THF (15 mL) was added dropwise in the stirred mixture solution at 0°C for 30 min and then at room temperature for 3 h. The solution was acidified with 10% HCl, extracted with EtOAc and

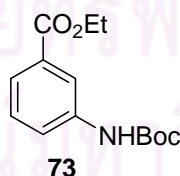
washed with sat. NaCl to give **72** (1.1518 g, quantitative yield) as white solid, R_f on TLC chromatogram= 0.50 (1:4 hexane:EtOAc), $^1\text{H NMR}$ (DMSO) (δ , ppm): 9.53 (s, 1H), 8.13 (s, 1H), 7.60 (d, $J=8.40$ Hz, 1H), 7.52 (d, $J=7.6$ Hz, 1H), 7.34 (t, $J=8$ Hz, 1H), 2.49 (s, 1H) (**Figure A.2**, Appendix).

2.3.2 Synthesis of ethyl-3-acetamidobenzoate **79** [56]



Acetyl chloride (5.00 mL, 57.59 mmol) was added dropwise in a solution of ethyl-3-aminobenzoate (0.1835 g, 1.11 mmol) in CH_2Cl_2 (5 mL). Then Pyridine (0.5 mL, 6.46 mmol) was added in the mixture. Reaction mixture was stirred on water bath under N_2 gas for 2.5 h, extracted with EtOAc, washed with 10% NaHCO_3 and sat. NaCl, and evaporated to give compound **79**, R_f on TLC chromatogram= 0.50 (1:2 hexane:EtOAc), $^1\text{H NMR}$ (CDCl_3) (δ , ppm): 7.85 (s, 1H), 7.81 (d, $J=8$ Hz, 1H), 7.65 (d, $J=8$ Hz, 1H), 7.41 (s, 1H), 7.27 (t, $J=8$ Hz, 1H), 4.24 (q, $J=7.2$ Hz, 2H), 2.07 (s, 3H), 1.26 (t, $J=7.2$ Hz, 3H) (**Figure A.3**, Appendix).

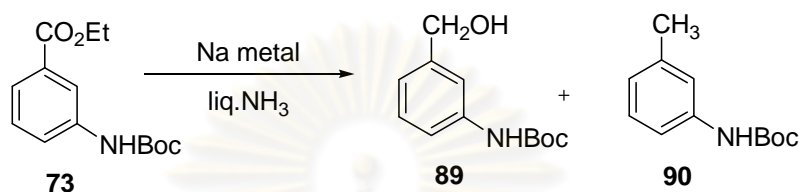
2.3.3 Synthesis of ethyl 3-(*tert*-butoxycarbonyl)benzoate **73** [44]



A solution of 0.7396 M of NaHCO_3 (13.2 mL, 9.76 mmol) was added ethyl-3-aminobenzoate (0.5382 g, 3.26 mmol). Boc_2O (2.25 mL, 9.79 mmol) in THF (13.23 mL) was added dropwise in the stirred mixture solution at 0°C for 30 min and stirred at room temperature for 20 h. Then, acidic with 10% HCl, extracting with EtOAc, washing with sat. NaCl gave **73** (79.80%) as white solid, R_f on TLC chromatogram= 0.50 (2:1

hexane:EtOAc), ^1H NMR (CDCl_3) (δ , ppm): 7.90 (bs, 1H), 7.70 (d, $J=7.6$ Hz, 2H), 7.35 (t, $J=7.6$ Hz, 1H), 6.65 (s, 1H), 4.36 (q, $J=7.2$ Hz, 2H), 1.51 (s, 9H), 1.37 (t, $J=7.2$ Hz, 3H) (**Figure A.4**, Appendix).

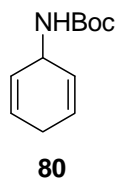
2.3.4 Birch reduction of **73** with Na metal [45]



Na metal (0.57 g, 24.8 mmol) was added in liquid ammonia under N_2 atmosphere at -78°C (dry ice-acetone bath). When the stirred changed into dark blue color, compound **73** in THF was added carefully. NH_4Cl was added until the solution turned yellow. The cooling bath was removed and allowed liquid ammonia to evaporate. Ice was added to destroy the leftover Na metal. The crude mixture was extracted with n-pentane and removed the solvent by rotary evaporator to give yellow liquid. Finally, purification through by column chromatography gave compound **89** (6.09%) and **90** (4.54%) on silica gel. ^1H NMR of **89** (400 MHz, CDCl_3) (δ , ppm): 7.38 (s, 1H), 7.20 (t, $J=8$ Hz., 1H), 7.14 (d, $J=8$ Hz., 1H), 6.97 (d, $J=10$ Hz., 1H), 6.43 (s, 1H), 4.60 (s, 2H), 1.45 (s, 9H) (**Figure A.5**, Appendix); ^1H NMR of **90**: 7.19 (s, 1H), 7.09 (t, $J=8$ Hz, 1H), 7.01 (d, $J=8$ Hz, 1H), 6.77 (d, $J=8$ Hz, 1H), 6.37 (s, 1H), 1.44 (s, 1H), 1.38 (s, 1H) (**Figure A.6**, Appendix).

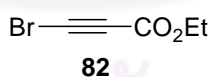
ศูนย์วิทยทรัพยากร
จุฬาลงกรณ์มหาวิทยาลัย

2.3.5 Birch reduction of **73** with Li metal [46]



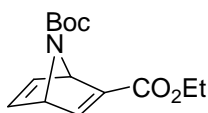
Li metal (1.94 g, 0.28 mol) was added in liquid ammonia under N₂ atmosphere at -78°C (dry ice-acetone bath). When the stirred changed into dark blue color, compound **73** was added carefully. Absolute ethanol (1 mL) was added after 10 min of stirring. After 3.5 h, NH₄Cl was added until the solution turned yellow. The cooling bath was removed and allowed liquid ammonia to evaporate. Ice was added to destroy the leftover Li metal. The crude mixture was acidified to pH 3 with 10% HCl, extracted with diethyl ether and removed the solvent by rotary evaporator to give yellow liquefied mixture. Finally, separation by column chromatography potentially gave compound **80** (15.77%) on silica gel, R_f on TLC chromatogram= 0.25 (4:1 hexane:EtOAc), ¹H NMR (400 MHz, CDCl₃) (δ, ppm): 5.80 (bs, 2H), 5.69 (bs, 2H), 3.61 (d, *J*=4 Hz, 2H), 2.76 (m, 2 H), 1.46 (s, 9H) (**Figure A.7**, Appendix).

2.3.6 Synthesis of ethyl 3-bromopropiolate **82** [48]



N-bromosuccinimide (7.19 g, 40.4 mmol) and AgNO₃ (0.62 g, 3.67 mmol) were added ethyl propiolate (3.71 mL, 36.6 mmol) in dry acetone (40 mL) and stirred for 2 h. Water (40 mL) was added and filtered off the insoluble solid. The filtered solution was extracted with hexane, washed with 10% HCl (4x20 mL), dried with anhydrous Na₂SO₄, and then evaporated the solvent to give **82** (46.78%) as light yellow liquid. ¹H NMR (400 MHz, CDCl₃) (δ, ppm): 4.18 (q, *J*=7.2 Hz, 2H), 1.26 (t, *J*=7.2 Hz, 3H) (**Figure A.9**, Appendix).

2.3.7 Synthesis of 7-Azabicyclo[2.2.1]hepta-2,5-diene-2,7-dicarboxylic acid, 7-(1,1-dimethylethyl) 2-ethyl ester **85 [49]**



85

Ethyl propiolate (0.50 mL, 4.93 mmol) was added 1-(tert-butyloxycarbonyl) pyrrole (3.384 mg, 20.25 mmol) heated at 70-75 °C for 1 day. The crude mixture was purified by column chromatography (15:1 hexane:Et₂O) to give 351 mg (2.67%) of **85** as yellow oil, R_f on TLC chromatogram= 0.4 (5:1 hexane:EtOAc). ¹H NMR(CDCl₃) (δ, ppm): 7.69 (bs, 1H), 7.15 (bd, *J*= 28 Hz, 1H), 6.97 (bd, *J*= 24.8 Hz, 1H), 5.40 (bs, 1H), 5.33 (bs, 1H), 4.21 (q, *J*= 6.8 Hz, 2H), 1.40 (s, 9H), 1.29 (t, *J*=7.2 Hz, 3H) (**Figure A.11**, Appendix).

2.4 Molecular docking study between proteins and ligands

2.4.1 Structure modeling of ligands

Molecular models of 32 oseltamivir analogs (cpds. ID **m1-m32**) and *D/L*-gabaculine (cpds.ID **m33-m34** as **Figure 2.1**), were built in its hydrolysis form at ethyl ester position which is known to be the active metabolite of oseltamivir (**Table 2.1**). In addition, ligands possessing amine groups were built as a protonated form. This model-built step was done using the program HyperChem version 6. Then the models were then geometrically optimized using the molecular mechanic (MM) force field available in the program HyperChem to obtain a proper shape of ligand molecules. Subsequently, the structure models were refined using quantum mechanical optimization (Hartree-Fock method) with 6-31G* basis set available in the program Gaussian [50]. After this step, the final structures of all ligands were obtained and used for molecular docking. Substituents and stereochemical configurations of the designed oseltamivir analogs were summarized in **Table 2.1**.

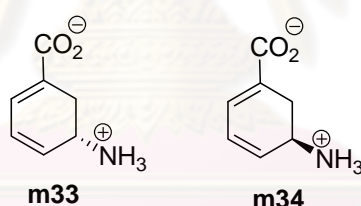
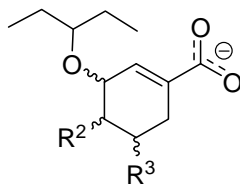


Figure 2.1 *D*-gabaculine (**m33**) and *L*-gabaculine (**m34**)

ศูนย์วิทยทรัพยากร
จุฬาลงกรณ์มหาวิทยาลัย

Table 2.1 Substituents and stereochemical configurations on oseltamivir analogs

Compounds ID	Configuration at C ₃	R ¹	Configuration at C ₄	R ²	Configuration at C ₅
m1	<i>R</i>	NHAc	<i>S</i>	NH ₃ ⁺	<i>S</i>
m2			<i>S</i>		<i>R</i>
m3			<i>R</i>		<i>S</i>
m4			<i>R</i>		<i>R</i>
m5	<i>S</i>		<i>S</i>		<i>S</i>
m6			<i>S</i>		<i>R</i>
m7			<i>R</i>		<i>S</i>
m8			<i>R</i>		<i>R</i>
m9	<i>R</i>	NH ₂	<i>S</i>	NH ₃ ⁺	<i>S</i>
m10			<i>S</i>		<i>R</i>
m11			<i>R</i>		<i>S</i>
m12			<i>R</i>		<i>R</i>
m13	<i>S</i>		<i>S</i>		<i>S</i>
m14			<i>S</i>		<i>R</i>
m15			<i>R</i>		<i>S</i>
m16			<i>R</i>		<i>R</i>
m17	<i>R</i>	NH ₃ ⁺	<i>S</i>	NH ₂	<i>S</i>
m18			<i>S</i>		<i>R</i>
m19			<i>R</i>		<i>S</i>
m20			<i>R</i>		<i>R</i>
m21	<i>S</i>		<i>S</i>		<i>S</i>
m22			<i>S</i>		<i>R</i>
m23			<i>R</i>		<i>S</i>
m24			<i>R</i>		<i>R</i>
m25	<i>R</i>	OH	<i>S</i>	NH ₃ ⁺	<i>S</i>
m26			<i>S</i>		<i>R</i>
m27			<i>R</i>		<i>S</i>
m28			<i>R</i>		<i>R</i>
m29	<i>S</i>		<i>S</i>		<i>S</i>
m30			<i>S</i>		<i>R</i>
m31			<i>R</i>		<i>S</i>
m32			<i>R</i>		<i>R</i>

In the study, two viral glycoproteins, neuraminidase (NA) and hemagglutinin (HA) were used as the target in molecular docking studies. However, only the crystal structure of neuraminidase-oseltamivir complex is available in Protein Data Bank. Therefore, the x-ray data of oseltamivir are useful for molecular docking simulations to serve as the reference model and the docking test for the NA system. In contrast, the 3D structure of hemagglutinin-drug complex from x-ray diffraction technique is not yet determined. Alternatively, the x-ray structure data of hemagglutinin-acetylneuraminic acid (or sialic acid receptor) were used for the docking of HA system.

For molecular docking of oseltamivir and sialic acid, the atomic coordinates of these two ligands were taken from the x-ray crystallographic data of neuraminidase-oseltamivir complex (PDB ID = 2HU4) and hemagglutinin-acetylneuraminic acid (PDB ID = 1JSN), respectively. Hydrogen atoms were added to these structure models which were subsequently optimized with 6-31G* basis set using the program Gaussian.

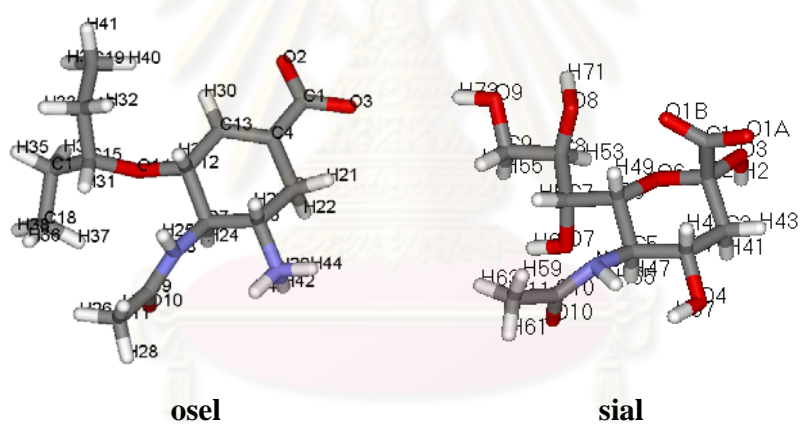


Figure 2.2 X-ray structure of oseltamivir (**osel**) and sialic acid (**sial**)

2.4.2 Structure modeling of proteins

The structural x-ray data used as protein models in molecular docking study were from two proteins; neuraminidase from the influenza virus strain A/VietNam/1203/2004/H5N1 and hemagglutinin from the influenza virus strain A/Duck/Singapore/3/1997/H5N3. The three-dimension structure of the studied proteins were downloaded from Protein Data Bank having PDB ID 2HU4 (resolution 2.5Å) [51] for neuraminidase N1 and 1JSN (resolution 2.4Å) [52] for hemagglutinin H5.

2.4.3 Molecular docking of N1 with oseltamivir and its analogs

In this study, the program AutoDock tools (ADT) [53] were used to set up Autodock input parameters for both the protein and ligands and Molecular docking runs were performed using the program Autodock 4.0 [54].

Initially, docking parameters, particularly choice of atomic charges, were tested by performing a series of Autodock runs of neuraminidase N1 and the reference oseltamivir carboxylate, of which the atomic positions of the ligand oseltamivir with respect to N1 is already known based on the x-ray structure. Hydrogen atoms were added to the x-ray structures of the protein and ligand as all hydrogen and polar hydrogen representation. The atomic charges of both the protein and ligand were assigned with Kollman's and Gasteiger's charge types. Thus, there were a total of four different dataset for Autodock runs. These include all atoms with Kollman's atomic charges, polar hydrogen with Kollman's united atomic charges, all atoms with Gasteiger's atomic charges and polar hydrogen with Gasteiger's united atomic charges. Hence, the data set of the test run that gave the best fit to experimental data were used for docking of N1 and the oseltamivir analogs and gabaculine. Moreover the number of docking run was varied between 100 to 1000 samplings to obtain the optimal sampling numbers of Autodock run that can give a reliability of the method.

For Autodock runs, a grid box of 90 x 90 x 90 lattice points with a spacing of 0.375 Å was constructed around the binding site of the oseltamivir-N1 complex. All rotatable bonds for the ligand were set to active for flexible docking. Grid center of the map was 84.467 -22.224 55.592 of xyz-coordinates (**Figure 2.3**). The Lamarckian genetic algorithm (LGA) procedure was employed and the docking runs were set to 500 samplings. The rest of the docking parameters were taken as default. The docking results obtained from Autodock were clustered based on conformational similarity, according to the atomic root mean square deviation (RMSD) tolerance (in Å unit) and ranked in order of the docking energy.

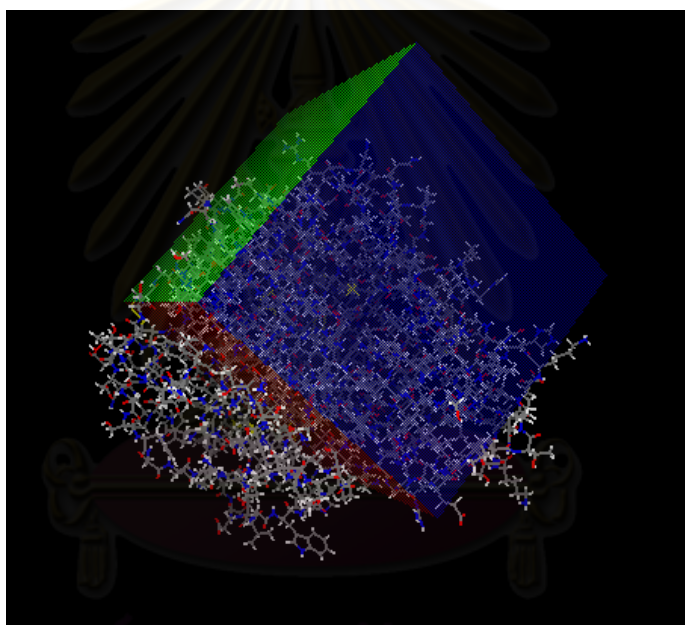


Figure 2.3 Grid box in neuraminidase docking

ศูนย์วิทยุทรัพยากร
จุฬาลงกรณ์มหาวิทยาลัย

2.4.4 Molecular docking of H5 with sialic receptor and its substrate analog inhibitors

Molecular docking of the hemagglutinin H5 protein target and sialic acid receptor (the reference structure) as well as its substrate analog inhibitors were carried out using the program Autodock 4.0. Hydrogen atoms were added to the x-ray structures of the protein and ligand. The structures of the protein target and ligands (in 2.4.1 and 2.4.2) were present as all atom models with Gasteiger charges (as described in 2.4.3).

For Autodock runs, a grid box of 90 x 90 x 90 lattice points with a spacing of 0.375 Å was constructed around the binding site of the oseltamivir-N1 complex. All rotatable bonds for the ligand were set to active for flexible docking. Grid center of the map was 84.467 -22.224 55.592 of xyz-coordinates. The Lamarckian genetic algorithm (LGA) procedure was employed and the docking runs were set to 500 samplings. The rest of the docking parameters were taken as default. The docking results obtained from Autodock were clustered based on conformational similarity, according to the atomic root mean square deviation (RMSD) tolerance (in Å unit) and ranked in order of the docking energy.



Figure 2.4 Grid box in hemagglutinin docking

2.4.5 Analysis of the docking results

Analysis of the docking results obtained from Autodock includes docking energy or binding free energy ($\Delta G_{\text{binding}}$), visual inspection, comparison of interactions between the ligand and the protein together with the cluster rank and the number of docked conformations in the cluster.

2.4.5.1 Docking energy

The binding free energy obtained from Autodock is a sum of individual scoring free energy terms as follows:

$$\Delta G_{\text{binding}} = \Delta G_{\text{vdW}} + \Delta G_{\text{elec}} + \Delta G_{\text{Hbond}} + \Delta G_{\text{desolv}} + \Delta G_{\text{tors}} \dots\dots\dots(1)$$

Where ΔG_{vdW} is 12-6 Lennard-Jones scoring potential (with 0.5 Å smoothing), ΔG_{elec} is the electrostatic scoring potential with Solmajer & Mehler distance-dependent dielectric, ΔG_{Hbond} is the 12-10 Hydrogen-bonding scoring potential, ΔG_{desolv} is the desolvation term and ΔG_{tors} is the empirically entropic scoring potential related to the number of rotatable bonds.

2.4.5.2 RMSD

The docked structures of ligands were also evaluated with the reference ligand structure (oseltamivir or sialic acid). For such assessment, the atomic root mean square deviation (RMSD) were calculated using eq(4).

$$RMSD = \sqrt{\frac{1}{N} \sum_{i=1}^{i=N} \delta_i^2} \dots\dots\dots(2)$$

2.4.5.3 Probability score

In this study, new scoring method was introduced for evaluating Autodock results. Previously introduced by Sotrifer et al [55], a modified probability score is computed in a form of an exponential function comparable to the Boltzmann. The two probability score were given as follows:

$$PSE = \frac{H_d}{H_{ref}} \exp(-\Delta E / wRT) \dots\dots\dots(3)$$

$$PSR = \frac{H_d}{H_{ref}} \exp(-R_{RMSD} / wRT) \dots\dots\dots(4)$$

$$\Delta E = E_{lig} - E_{ref}$$

Where *PSE* is the energy-based probability score, *PSR* is the distance-based probability score, ΔE is the difference in docked energy between ligand-protein and the reference complexes (N1-**osel** or H5-**sial**). H_d is the number of docked conformations in the cluster, H_{ref} is the number of docked conformations in the cluster of the reference ligands (**osel** or **sial**), R is the gas constant ($1.98719 \text{ cal K}^{-1} \text{ mol}^{-1}$), T is 289.15 K, and R_{RMSD} is the atomic root mean square deviation of the selected atoms from the selected conformation of protein-ligand docking with respect to the compared atoms from the selected conformation of protein-reference ligand docking, w is weighting factor. The comparison of docking energies with free energies of binding indicated that they differ by one order of magnitude. Thus this factor was assigned 10.

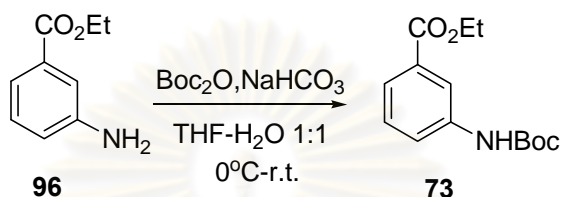
On the basis of Eq(3) and Eq(4), *PSE* is a probability score based on energy comparison between the protein-ligands and the reference complexes. By analogy, *PSR* is a probability score based on the position difference between the ligand and reference ligand atoms.

CHAPTER III

RESULTS AND DISCUSSION

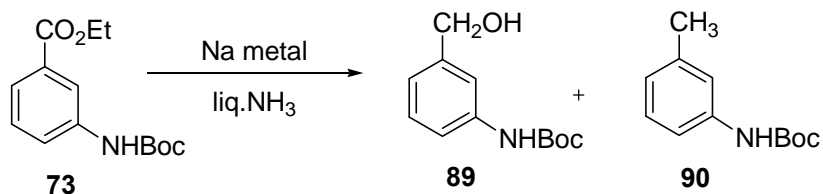
3.1 Birch reduction of 3-aminobenzoic acid derivatives

Table 3.1 Protection of amine group of **96**



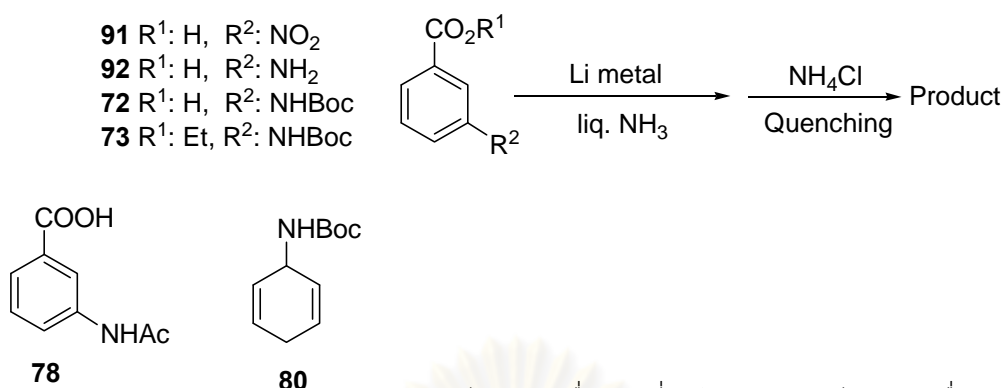
Entry	NaHCO ₃ (eq.)	(Boc) ₂ O (eq.)	Time (h)	%yield
1	3.0	3.0	3	61
2	3.0	3.0	20	80
3	1.5	1.5	54	78
4	2.0	1.5	54	76
5	2.5	1.5	54	76
6	1.5	1.5	3	69
7	1.0	1.5	44	87

Compound **96** was protected at the amine group to yield up to 87% of **73** following the method reported by Shendage et al. [56]. The yield of **73** tended to increase with longer reaction time (**Table 3.1**, Entry 2). The invariance of the %yield of **73** in Entry 3 – Entry 5 suggested that the concentration of NaHCO₃ may not significantly affect the reaction. When the reaction was scaled down, while keeping the ratio of NaHCO₃:(Boc)₂O, %yield of **73** was increased from 61% to 69% (Entry 1 and Entry 6, respectively). The maximum yield of **73** was achieved when the concentration (eq.) of NaHCO₃ was equaled to the starting material **96** (Entry 7). The protection of the amine group of **96** with the proposed reaction was one of the potential methods for preparing the starting material **73** for subsequent reactions. The %yield of the reaction was good (up to 87%) with the smaller scale of starting materials (**96**, NaHCO₃, and (Boc)₂O). The optimal reaction time was a little bit longer than the reported methods [57, 58]. The product was used as the starting material in the subsequent Birch reduction steps.

Table 3.2 Birch reduction of **73** with Na metal

Entry	Na(eq.)	Time	Quenching agent	Extraction	Product
1	3.0	10 min	MeOH	Et ₂ O	89 (0.32%)
2	3.0	20 min	NH ₄ Cl	n-pentane	No reaction
3	13.5	1 h	NH ₄ Cl	n-pentane	89 (6.09%), 90 (4.54%)

The starting material **73** underwent Birch reduction with Na metal at the substituted ester groups. The products **89** and **90** were obtained among other unidentified mixture (**Figure A.5** and **Figure A.6**, appendix). The chemical shift at 4.0 ppm 1.9 ppm and 1.2 ppm in NMR spectrum of **89** was attributed to leftover hexane and ethyl acetate used in the column chromatography. MeOH was presumed to accelerate the rearomatization of the pre-formed products as same **73** was recovered (Entry 1). Alternatively, NH₄Cl was used as the quenching agent instead for some subsequent attempts (Entry 2 and Entry 3). In order to suppress the possible side reactions, *n*-pentane was employed as the extracting solvent. Unfortunately, the Birch reduction with Na metal didn't seem to be able to reduce the aromatic core of **73** under the condition used. Only some side chain reductions were found in one of the attempts.

Table 3.3 Birch reduction with Li metal

ผิดพลาด! ไม่ใช่การเชื่อมโยงที่ถูกต้องผิดพลาด! ไม่ใช่การเชื่อมโยงที่ถูกต้อง

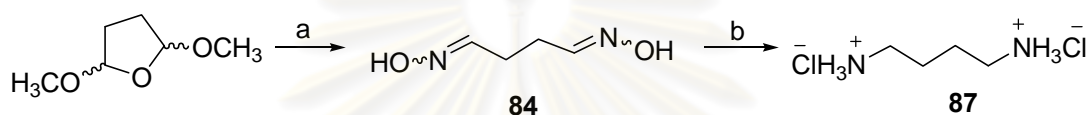
Entry	Starting material (mmol)	Li (eq.)	Ethanol (mL)	Time (h)	Product
1	91 (14.62)	14.8	5	5	78
2	92 (1.33)	108.3	2	2	No reaction
3	72 (0.84)	257.3	1	2	No reaction
4	73 (1.89)	114.4	5	3	No reaction
5	73 (1.01)	271.1	2	4	Mixture of aromatic products
6	73 (1.33)	175.5	0	4	No reaction
7	73 (1.03)	271.4	1.5	3.5	80

After the failure of the Birch reduction with Na metal and Li metal was employed as an alternative. Birch reduction of **91** with Li metal (Entry 1) yielded the unextractable product in organic phase. Part of the nitro group of **91** was reduced to amino group and which was verified by further acetylation of the product to yield compound **78**. No reaction was observed after 2 hrs when compounds **92** and **72** were used as the starting materials (Entry 2 and Entry 3). Compound **80** were potentially obtained among a few isolable products when **73** was used in several attempts (Entry 7).

In most cases, the reaction yielded rather complicate mixture of many compounds. After attempted chromatographic separations, the isolated products didn't seem to fit with any compounds expected from straightforward Birch reduction. One of the compounds, which were postulated to be compound **80**, was among a few products obtained cleanly enough to be identified. However the mechanistic route for its formation that possibly involved one-carbon degradation was still unknown.

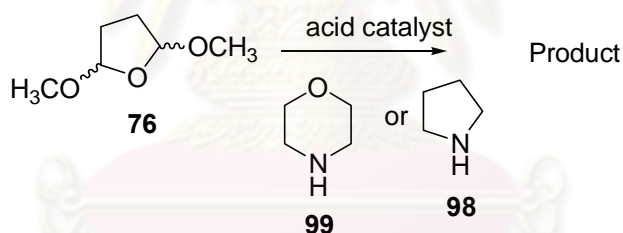
3.2 Synthesis of dienamine from 2,5-dimethoxy tetrahydrofuran

In principle, the ring opening reaction of 2,5-dimethoxy tetrahydrofuran can be carried out in an acidic medium to yield a dialdehyde compound. The imine ion can be formed from the condensation of dialdehyde and amine, which subsequently tautomerize to enamine. Frydman and coworkers [59] reported that putrescine dihydrochloride **85** could be prepared in 50% overall yield from 2,5-dimethoxytetrahydrofuran. The precursor was ring-opened in acidic medium and the resulting succinic dialdehyde was trapped as its dioxime **84**, which was then reduced to **85** (Scheme 3.1).



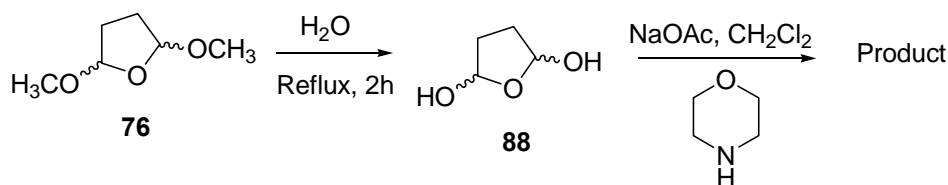
a: i) 50% AcOH, 1h, 80°C; ii) HONH₂·HCl, NaOAc, 24h, 20°C; iii) ext. EtOAc
 b: i) 50% Reney Ni, 2N NaOH/EtOH 1:1, 2h, 25°C; ii) ext. CHCl₃; iii) CH₃OH/HCl

Scheme 3.1 Dioxime from trapped succinic dialdehyde



Scheme 3.2 The condensation reaction of **76** and secondary amine

When we carried out the condensation reaction with acid catalyst (such as AcOH 50%, conc. AcOH, TFA) and secondary amines as in **Scheme 3.2**, however, only unidentified insoluble colored mixture, assumed to be a kind of polymer, was formed.



Scheme 3.3 The condensation reaction of hydrolyzed **76**

Since amine compounds were highly susceptible to decompositions, great care should be kept in mind when the reaction was carried out in acidic medium at elevated temperature. Gourlay and coworkers [60] developed a new route that could be carried out in acetate buffer at pH 5 as shown in **Scheme 3.3**. Compound **76** was subjected to the hydrolysis in water and the diacetal was formed. The diacetal could react in the subsequent steps to give the dienamine was formed. As we followed such procedure, only small amount of the possible dienamine compound **97** from the condensation with morpholine could be identified out of the crude product (**Figure 3.1**).

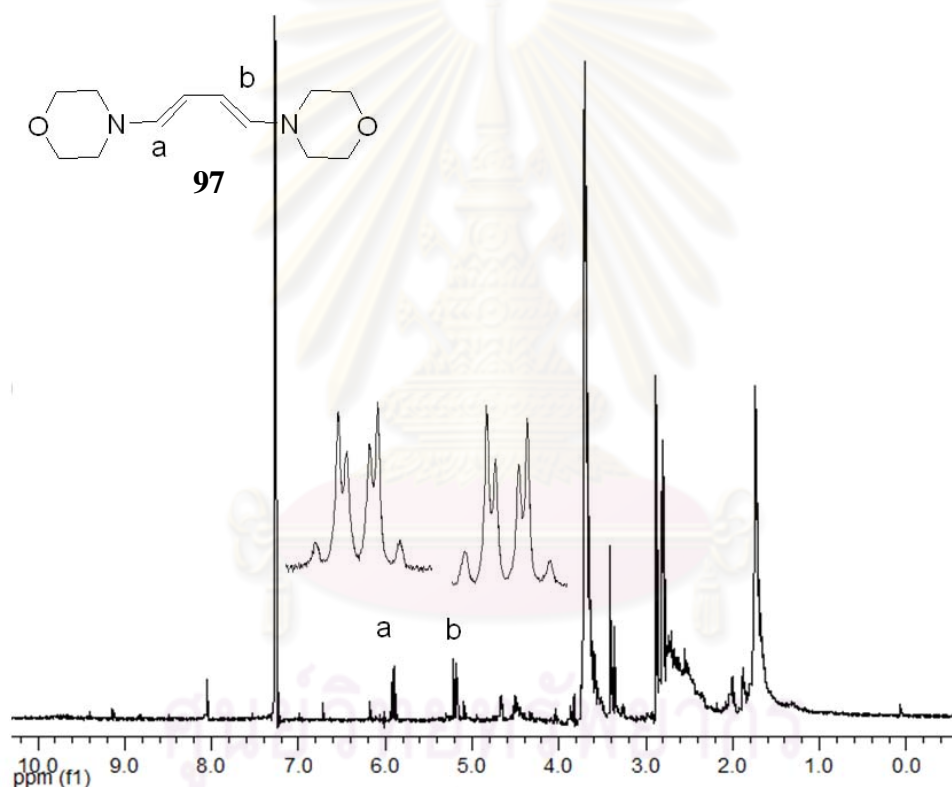


Figure 3.1 ^1H NMR spectra of dienamine **97**

From **Figure 3.1**, the characteristic splitting patterns of protons a and b at chemical shift 5.9 and 5.2, respectively, indicated the presence of diene moiety from the condensation reaction into a dienamine. Since the dienamine product was probably highly reactive at ambient condition, in situ reaction with ethyl acrylate was attempted. However, no addition product was observed. We anticipated that small amount of the diene and residual water in the mixture might retard or prevent the

condensation reaction. In one of the experiments, we only observed compound **81** as the only isolable product, possibly obtained from the known Michael addition of the leftover pyrrolidine, used as the amine precursor, onto the added ethyl acrylate (**Figure A.8**, Appendix).

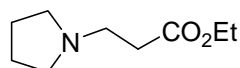
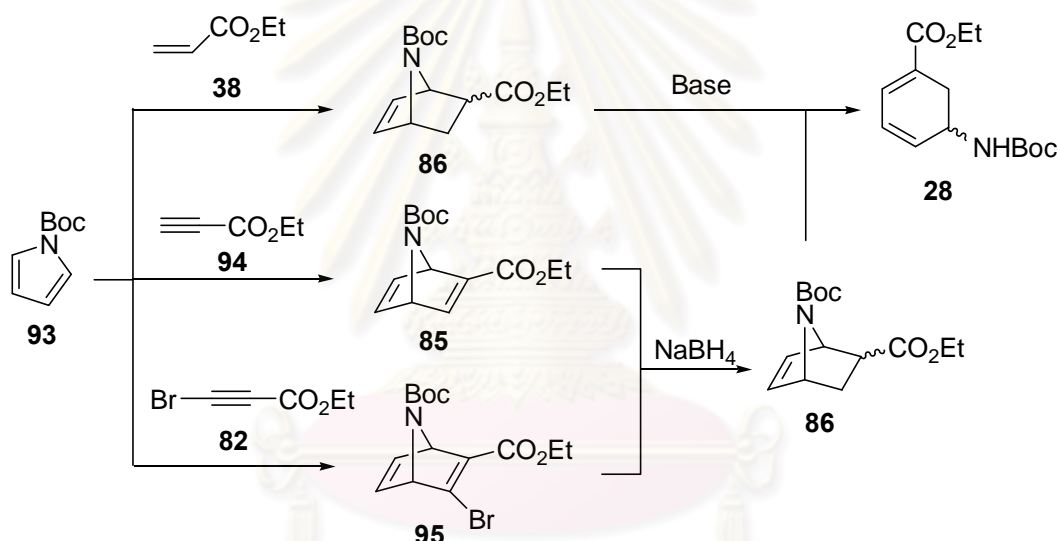


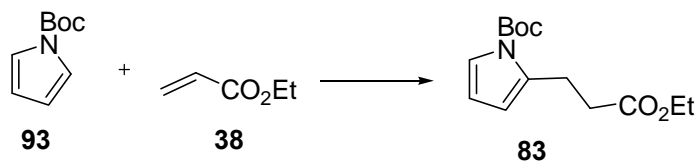
Figure 3.2 Structure of 1-pyrrolidinepropanoic acid **81**

3.3 Diels-Alder reaction of 1-(*tert*-butyloxycarbonyl)pyrrole



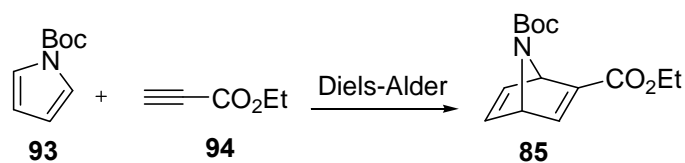
Scheme 3.4 Synthesis of gabaculine via Diels-Alder and reduction reactions

The synthesis of gabaculine via Diels-Alder reaction was proposed through 3 dienophiles (**Scheme 3.4**). The resulted bicycles were expectedly subjected to ring-opening with strong base. In the first step, cycloaddition reactions between **95** and **38** were attempted with no success (**Table 3.4**). Lewis acids or varying temperature did not seem to help generating the target molecule. In an instance, (Entry 4) side product **83** was obtained instead, possibly through the Michael addition of the starting materials. In other cases where the reactions did take place, it was assumed that polymerizations of **93** of either **38** or both had predominated [61].

Table 3.4 The first Diels-Alder reaction pathway of **93**

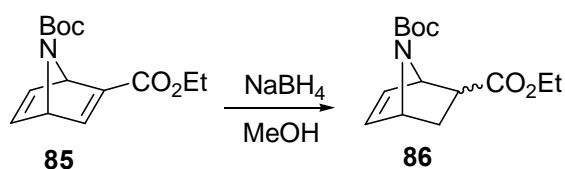
Entry	93 (mmol)	38 (mmol)	Catalyst (eq)	Solvent	Temperature (°C)	Time	Product
1	1.50	1.75	-	-	60-85	58 h	No reaction
2	4.98	2.49	AlCl ₃ (1)	CH ₂ Cl ₂	r.t.	62 h	Black gum
3	3.17	6.34	AlCl ₃ (0.5)	CH ₂ Cl ₂	0-r.t.	38.5 h	No reaction
4	3.44	6.88	ZnCl ₂ (1)	CH ₂ Cl ₂	0-r.t.	4 days	83
5	3.23	6.89	ZnCl ₂ (1)	-	55	2 min	Black brown gum

The Diels-Alder reaction of **93** and **94** showed a little better sign (**Table 3.5**), giving low yield of **85**. Temperature, time or starting materials ratio variations didn't help improve the result. The presence of ZnCl₂ (Entries 6, Entries 7) also led to polymerizations of either starting material, similarly to the previous cycloadditions. The weaker Zn(OAc)₂ (Entry 8) did not catalyze the reaction at all.

Table 3.5 The second Diels-Alder reaction pathway of **93**

Entry	93 (mmol)	94 (mmol)	Condition	Product (Yield)
1	11.52 (4.3 eq)	2.66	85°C, 24 h	85 (2.1%)
2	49.34 (4.0 eq)	12.33	75-85°C, 2 days	85 (1.1%)
3	19.83 (4.0 eq)	4.93	65-75°C, 2 days	85 (1.3%)
4	19.88 (3.4 eq)	5.92	70-75°C, 1.5 days	85 (3.4%)
5	19.83 (4.0 eq)	4.93	65-75°C, 2 days	85 (1.3%)
6	39.48 (4.0 eq)	9.87	ZnCl ₂ 1 eq, r.t. -75°C	Black gum
7	31.09 (3.1 eq)	9.87	ZnCl ₂ 11%mol, 0°C (6 h), r.t. (1-4 days)	black solid
8	19.99 (4.0 eq)	4.93	Zn(OAc) ₂ 13.59 %mol, 60°C, 3 days	No reaction

Reduction of **85** with NaBH₄ in MeOH to give **86** was carried out following the protocol reported by Lin et al. [62] Because of the very small amount of **85** obtained from the previous step, only few small scale reactions could be performed. The ¹H-NMR spectrum of one of the resulted crude products (**Figure 3.4**) appeared to have some signals that might correspond to part of the structure of **86**. Due to their tiny amount among many other side products in the mixture, its isolation was not pursued.

**Scheme 3.5** The reduction of **85** with NaBH₄

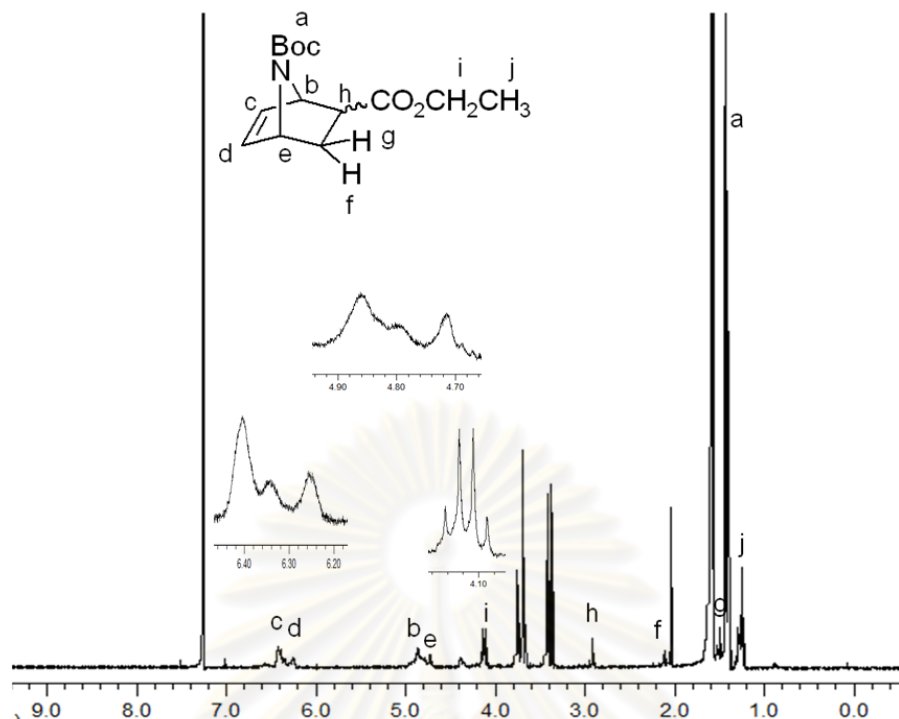
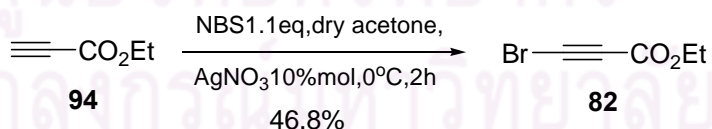
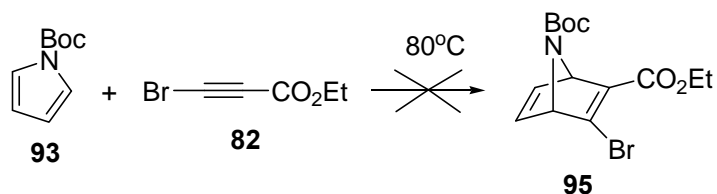


Figure 3.3 ^1H NMR spectrum of **86** in a crude mixture

Finally, the third cycloadditions between compounds **82** and **93** were attempted following what had been already described in the literature [63]. The synthesis of **82** was accomplished using the reported protocol [48], albeit with only moderate yield of 46.8 % (**Scheme 3.6**). Compound **82** has a highly eye-irritating, volatile nature and was needed to prepare right before use. Because of such inconvenience in its handling, the subsequent cycloaddition of **82** was carried out only once and was not yet successful (**Scheme 3.7**). The experiment was eventually terminated because a similar strategy has just been published [64].



Scheme 3.6 The terminal bromination of ethyl propiolate **94**



Scheme 3.7 The Diels-Alder reaction of **93** and **82**

3.4 Prediction test by Autodock

Initially, types of partial atomic charges, structure representation and number of trials in each Autodock run were examined with the known x-ray structure. This control step was performed to ensure that the Autodock parameters have been optimized for prediction of ligand binding study.

3.4.1 Atomic charges and structure presentation

Table 3.6 shows Autodock results in terms of Autodock mean energy and RMSD of the first rank (Lowest E) and the most populated configurations (highest frequency). The runs were varied by atomic charges of N1 and oseltamivir, in which the protein and ligand structures had different structure representation in terms of hydrogen attached to the heavy atoms (see method). As shown in **Table 3.6**, Docking with Gasteiger's charges always gave better results in terms of energy than docking with Kollman's charges. The mean energy of the All-H (7.90 kcal/mol), Polar-H (8.00 kcal/mol) and Merge non-polar-H (7.99 kcal/mol) structure presentation using Gasteiger's charges was essentially similar and greater than that of the Non-H (6.77 kcal/mol) structure representation. The experimental K_i data of oseltamivir-1 was 0.32 nM. Therefore, ΔG of binding corresponds to -12.93 kcal/mol at 298.15K. Additionally, using Gasteiger charges provided the first rank having the most populated configurations, except for the Non-H system. Therefore, the use of Kollman's atomic charges and the Non-H structure representation for the N1-Osel structure were not appropriate for the study.

The energy-frequency analysis together with RMSD data gave a clear indication about the best choice of atomic charges and structure presentation for the molecular docking study. The energy-frequency analysis described above has made the next consideration to focus on the docking results of the All-H, Polar-H and Merge non-polar-H structure representation using Gasteiger's charges, with which the RMSD values relative to the x-ray reference were 0.23, 0.31 and 0.49 Å, respectively. Thus, this can be concluded that the All-H structure representation and Gasteiger's charges were the best choice of the protein-ligand parameters for the study. Details of neuraminidase and oseltamivir structure and Gasteiger charges were shown in the appendix.

Table 3.6 Autodock mean energy and RMSD of the first rank (lowest E) and the most populated configurations (highest frequency) for N1-Osel docking

Charge	Docking results	Mean energy (kcal/mol) (frequency)				RMSD (Å)			
		All H	Polar H	Merge non-polar H	Non H	All H	Polar H	Merge non-polar H	Non H
Kollman's charge	Lowest E	-6.15 (73)	-5.95 (74)	-5.89 (77)	-	0.21	0.23	0.38	-
	Highest frequency	-4.61 (124)	-4.56 (133)	-4.62 (133)	-	4.06	4.05	4.05	-
Gasteiger's charge	Lowest E	-7.90 (221)	-8.00 (229)	-7.99 (199)	-6.77 (55)	0.23	0.31	0.49	1.11
	Highest frequency				-6.36 (219)				0.45

ศูนย์วิทยทรัพยากร
จุฬาลงกรณ์มหาวิทยาลัย

3.4.2 Number of trials in each Autodock run

A total of ten Autodock runs were performed by varying the number of trials from 100 to 1000. The results of each run were chosen for the analysis if the RMSD cutoff is less than 1 Å, a typical value to indicate a similarity of the compared structure. Therefore, the use of the RMSD cutoff is to identify the success rate of the run which was here reported as:

$$\%frequency = \frac{\text{The number of populated configurations under the cutoff}}{\text{The number of trials in each run.}}$$

Table 3.7 showed number of frequency (the number of populated configurations), %frequency, the mean energy and the RMSD relative to the x-ray reference. It should be noted that the success rate of the test was in a range from 10.5% to 19%. A range of the mean energy were -7.88-8.53 kcal/mol and the RMSD were 0.25-0.45 Å. From **Table 3.7**, three output parameters, %frequency, the mean energy and RMSD were used to determine the number of trials to be used for the next docking study

Table 3.7 Frequency, mean energy and RMSD from different number of trials in each Autodock run

Number of trials	frequency	%frequency	Mean energy (kcal/mol)	RMSD (Å)
100	19	19.0	-7.88	0.45
200	23	11.5	-8.25	0.41
300	38	12.7	-8.42	0.40
400	76	19.0	-8.42	0.36
500	79	15.8	-8.46	0.25
600	63	10.5	-8.53	0.39
700	89	12.7	-8.35	0.25
800	106	13.3	-8.46	0.35
900	118	13.1	-8.41	0.29
1000	148	14.8	-8.44	0.28

Table 3.8 %frequency, the mean energy and RMSD were individually ranked versus the number of trials. Note that the most preference choice here is the run that will give the results with the highest frequency, the lowest mean energy and the lowest RMSD. Considering data in **Table 3.8** provided the number of 500 trials to the optimum value not only in a sense of the docking results but also the statistical relevant.

Table 3.8 Rank of number of run from RMSD, mean energy and %frequency

RMSD (Å)	Number of trials	Mean energy (kcal/mol)	Number of trials	%frequency	Number of run
0.25	700	-8.53	600	19.00	100
0.25	500	-8.46	500	19.00	400
0.28	1000	-8.46	800	15.80	500
0.29	900	-8.44	1000	14.80	1000
0.35	800	-8.42	300	13.25	800
0.36	400	-8.42	400	13.11	900
0.39	600	-8.41	900	12.71	700
0.40	300	-8.35	700	12.67	300
0.41	200	-8.25	200	11.50	200
0.45	100	-7.88	100	10.50	600

3.5 Binding prediction of oseltamivir analogs

Binding mode prediction of 34 oseltamivir analogs within N1 binding site was analyzed. All the raw data used for plotting the graphs in discussion can be found in Appendix. From Autodock output, binding energies of the first rank (lowest energy) and the most populated configurations (highest frequency) were taken into consideration. Energy difference in binding energy between the analog docking and oseltamivir docking was computed as follows:

$$\Delta E = E_{\text{lig}} - E_{\text{ref}}$$

Where E_{lig} is docking energy of N1-ligand complex (the analog) taken from the first rank and the most populated configurations and E_{ref} is docking energy of N1-oseltamivir complex. The E_{ref} value was -8.46 kcal/mol (taken from the Autodock test with 500 trials). The energy differences of 34 analogs were shown in **Figure 3.4** (the first rank) and **Figure 3.5** (the highest frequency). It appears that the binding energy of **m24** is 0.55 kcal/mol lower than that of oseltamivir. The success rate of docking is almost 50%.

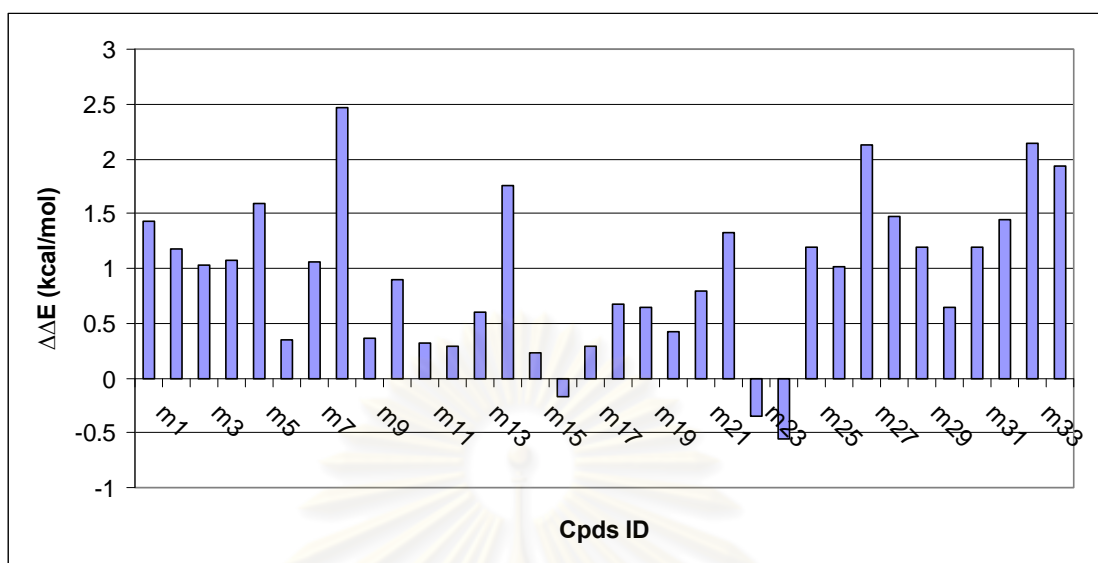


Figure 3.4 $\Delta\Delta E$ obtained from the lowest energy cluster of 34 analogs

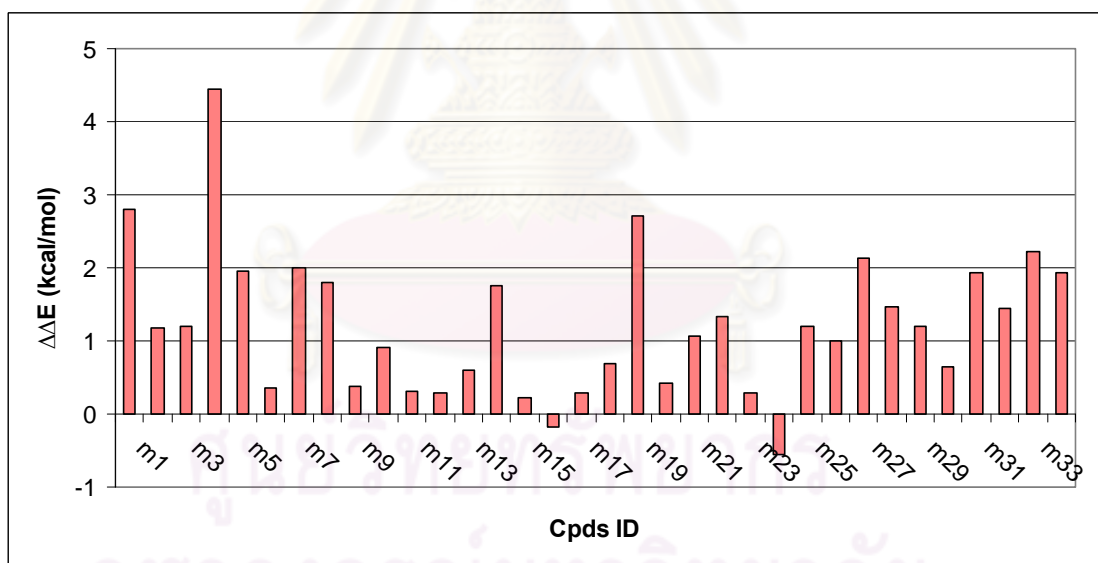


Figure 3.5 $\Delta\Delta E$ obtained from the highest frequency cluster of 34 analogs

A comparison of cyclohexadienyl position between the analogs and oseltamivir reference was performed by calculating the root mean square deviation of (six carbons in the central ring) denoted as RMSDcore. The calculated RMSDcore of 34 analogs were

summarized as following. $\text{RMSD}_{\text{core}} \leq 1\text{\AA}$ were from the docking of **osel**, **m6**, **m32**, **m2**, **m24**, **m16**, **m22**, **m20**, **m29**, **m14**, **m34**, **m26**, **m18**, **m30**, **m19**, **m12**, **m11** and **m28**. $1\text{\AA} < \text{RMSD}_{\text{core}} \leq 1\text{\AA}$ were from the docking of **m10**, **m1**, **m23**, **m7**, **m33**, **m21**, **m31**, **m5**, **m27**, **m25** and **m3**. $\text{RMSD}_{\text{core}} > 3\text{\AA}$ were from the docking of **m15**, **m17**, **m9**, **m13**, **m4** and **m8**. $\text{RMSD}_{\text{core}}$ of 34 analogs were plotted versus ΔE obtained previously. The results were shown in **Figure 3.6** (the first rank). By providing low $\text{RMSD}_{\text{core}}$ and ΔE values, the analog **m24** and **m16** were good candidates.

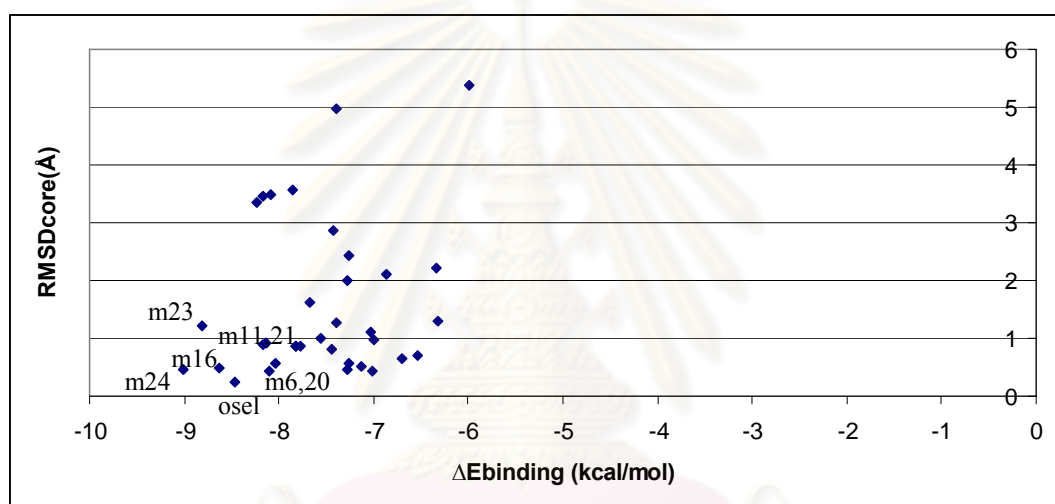


Figure 3.6 ΔE and $\text{RMSD}_{\text{core}}$ obtained from the lowest energy cluster of 34 analogs

Additional evaluation of the docking of 34 analogs was carried out by introducing probability score. Two types of the probability score were introduced in the study, PSE and PSR. Using the Boltzmann equation as described in the method and ΔE and $\text{RMSD}_{\text{core}}$ obtained from previous results, *PSE* and *PSR* were computed and shown in **Figure 3.7** in (the first rank). From the graph, the docking of **m34** and **m33** analogs (gabaculine) were the two greatest scores. However, the docking energies of these two analogs were slightly greater than that of oseltamivir, suggesting a weaker binding to N1 about 0.64 and 1.2 kcal/mol. These two analogs had the great success rate of docking indicated by %frequency which was used as a weighting factor in probability score function.

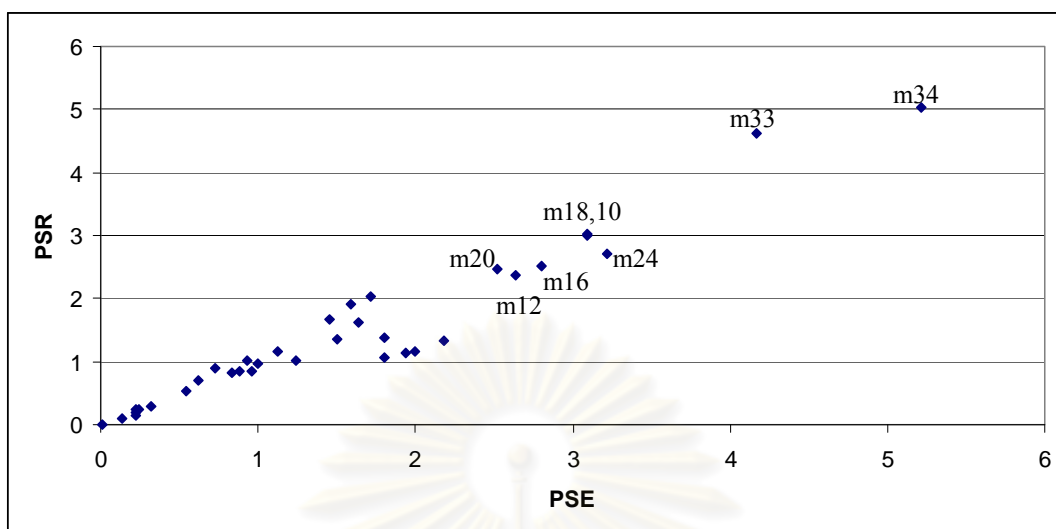


Figure 3.7 PSE vs PSR obtained from the lowest energy cluster of 34 analogs

Figure 3.8 showed structure of the analogs **m16**, **m24**, **m33** and **m34**. It appears that the structures of **m16** and **m24** shared common structural and chemical features. Both are composed of *S*-pentylether, *R*-NH₂ and *R*-NH₃⁺.

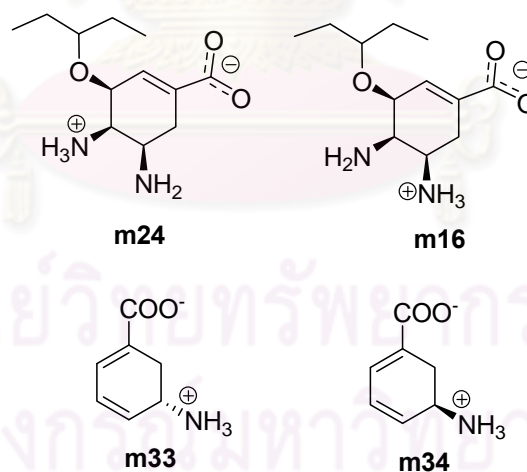


Figure 3.8 Structures of **m24**, **m16**, **m33** and **m34**



Figure 3.9 Binding of **m24** and NA

Table 3.9 H-bond of potential compounds

Cpds	ARG 118	GLU 119	ASP 151	ARG 152	GLU 277	ARG 292	ARG 371	TYR 406
osel		/	/	/		/	/	/
m24	/	/			/	/	/	/
m16		/	/			/	/	/
m33	/	/	/			/	/	/
m34	/				/	/	/	/

Based on the analysis described above, the **m24** analog has been of interest. The molecular docking of this analog exhibited 0.55 kcal/mol lower than the oseltamivir docking energy and achieved the binding configuration below the RMSD cutoff with the 50% success rate. From the analysis of the binding mode prediction, the **m24** analog could form hydrogen bonding with surrounding residues including ARG118, GLU119, GLU277, ARG292, ARG371 and TYR406 (**Table 3.9** and **Figure 3.9**).

Although, there is the significantly different of stereochemistry between x-ray and docking structure of oseltamivir, the superimposition of both structures shows that the position of the 3-pentyl ether is near because of the distortion of that functional group as shown in **Figure 3.10**.

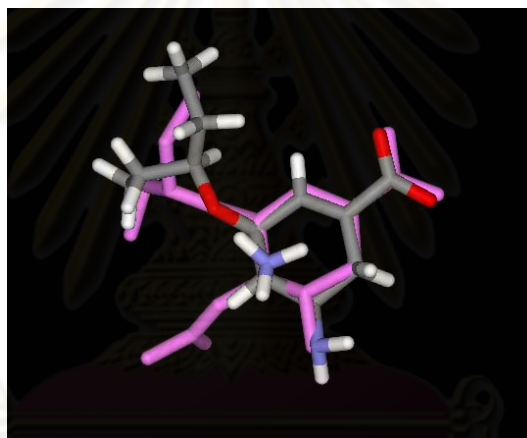


Figure 3.10 The superimposition between **m24** and x-ray structure of oseltamivir (pink)

ศูนย์วิทยทรัพยากร
จุฬาลงกรณ์มหาวิทยาลัย

3.6 Binding prediction of oseltamivir analogs to hemagglutinin

Binding mode prediction of 34 oseltamivir analogs within hemagglutinin binding site was analyzed. **Figure 3.11** showed ΔE and $\text{RMSD}_{\text{core}}$ obtained from the lowest energy cluster of 34 analogs. It appears that none of the analogs was found in the hemagglutinin binding site as shown by large values of $\text{RMSD}_{\text{core}}$. This indicated that these analogs may not be able to bind within hemagglutinin binding site or the present model of these analogs used for docking with neuraminidase cannot be used with hemagglutinin.

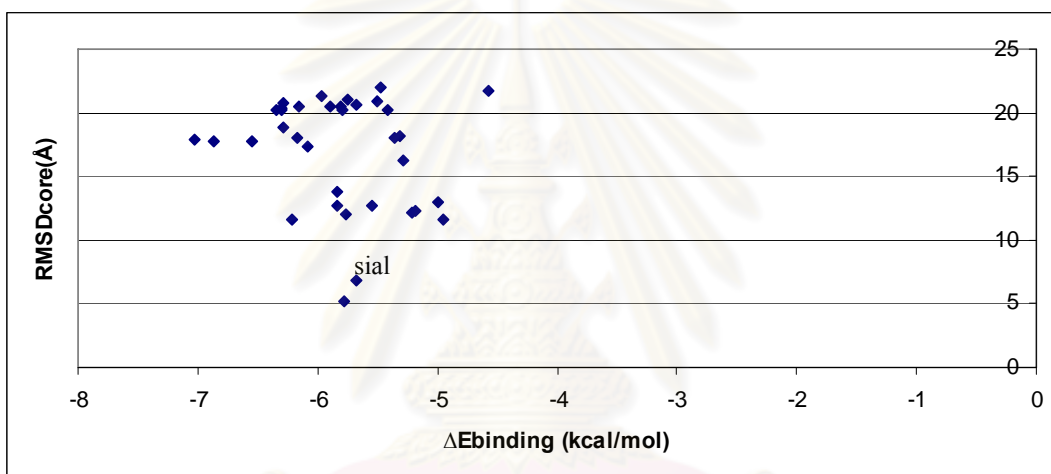


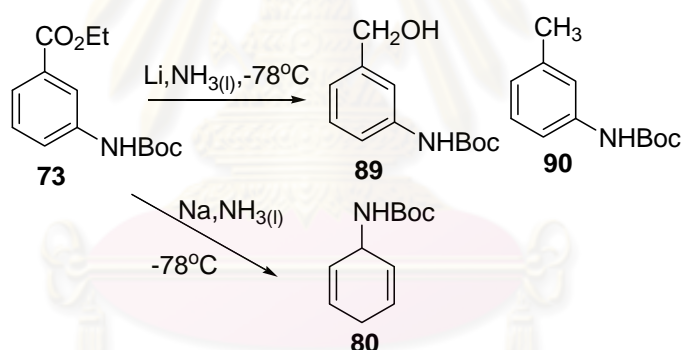
Figure 3.11 ΔE and $\text{RMSD}_{\text{core}}$ obtained from the lowest energy cluster of 34 analogs

ศูนย์วิทยทรัพยากร
จุฬาลงกรณ์มหาวิทยาลัย

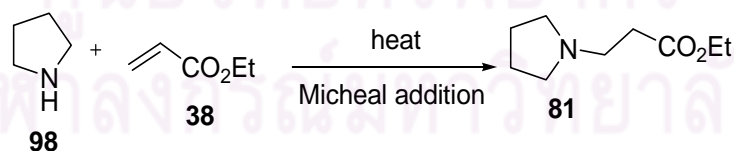
CHAPTER IV

CONCLUSIONS

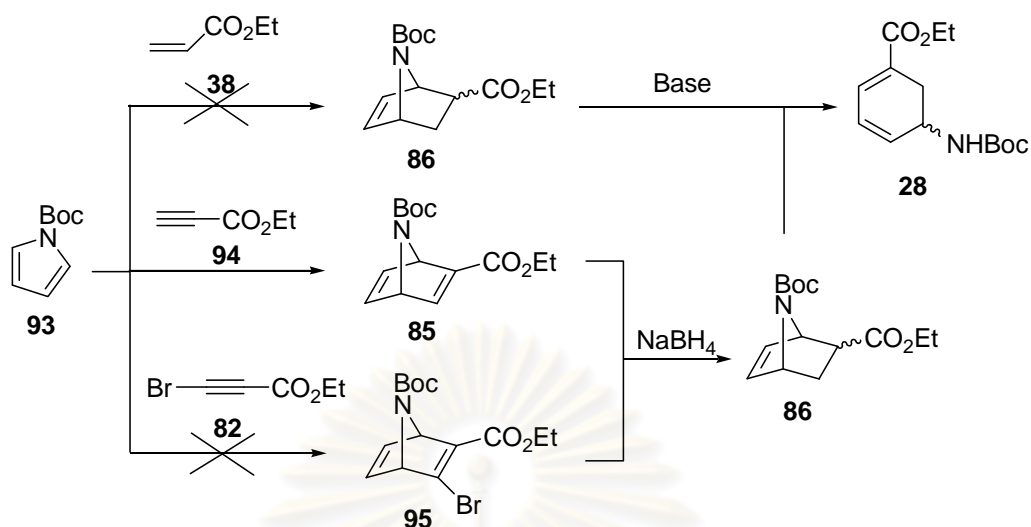
Synthesis of gabaculine derivatives, the intermediate towards synthesis of oseltamivir phosphate or Tamiflu[®] was carried out via many strategies. The Birch reduction using either Na or Li metal failed to give the desired gabaculine isomer (**Scheme 4.1**). The condensation of a secondary amine and succinic diacetal to create the diene precursor for subsequent Diels-Alder reaction only afforded unidentifiable polymeric products in most case. A side reaction from Michael addition of the two starting materials was detected as shown in **Scheme 4.2**. The direct cycloaddition on Boc-pyrrole gave the azabicyclic **85** when **94** was used as the dienophile, though in rather low yield of 3.4% (**Scheme 4.3**).



Scheme 4.1 Birch reduction of protected amonobenzoate **73**



Scheme 4.2 A side reaction during a condensation attempt



Scheme 4.3 The direct cycloaddition of **93**

The synthesis of gabaculine derivatives has led to the design of 34 oseltamivir-like structures for the prediction of the influenza viral protein binding site. The binding prediction of the neuraminidase inhibitors revealed that 17 analogs exhibited a similar orientation of cyclohexadienyl core structure compared to the X-ray crystal structure [51], but only two analogs were energetically favorable. Analysis of relative binding energy and position of ligand with respect to the binding pocket as the reference has suggested specific suitable stereoconfigurations and functional groups for the potential neuraminidase inhibitors. These analogs composed of (*S*)-pentylether group at C3 position and either (*R*)- NH_2 or (*R*)- NH_3^+ at C4 and C5 positions respectively on the 1-carboxy-cyclohexadienyl core structure. On the contrary, molecular docking of the analogs to hemagglutinin binding site revealed none of the ligand analogs was able to interact with the residues in the hemagglutinin binding pocket. The present model may not be suitable for this system. The predictive ability of molecular docking study depends on the interplay of the most likely local and global conformation of the bound ligand.

REFERENCES

- [1] Taubenberger, J. K.; Reid, A. H. and Fanning, T. G. The 1918 influenza virus: a killer comes into view. Virology 274 (2000): 241-245.
- [2] Wang, G. Recent advances in the discovery and development of anti-influenza drugs. Expert Opin. Ther. Pat. 12 (2002): 845–861.
- [3] Klumpp, K. Recent advances in the discovery and development of anti-influenza drugs. Expert Opin. Ther. Pat. 14 (2004): 1153–1168.
- [4] Laver, W. G.; Bischofberger, N. and Webster, R. G. Disarming flu viruses. Sci Am. 280 (1999): 78-87.
- [5] Trifonov, V.; Khiabani, H. and Rabadan, R. Geographic dependence, surveillance, and origins of the 2009 influenza A (H1N1) virus. N. Engl. J. Med. 361 (2009): 115-119.
- [6] WHO. Influenza virus [online]. Available from: http://www.who.int/csr/don/2009_04_24/en/index.html [2010, August 17].
- [7] Palese, P.; Tobita, K.; Ueda, M. and Compans, R. W. Characterization of temperature-sensitive influenza virus mutants defective in neuraminidase. Virology 61 (1974): 397-410.
- [8] Liu, C.; Eichelberger, M. C.; Compans, R. W. and Air, G. M. Influenza type A virus neuraminidase does not play a role in viral entry, replication, assembly, or budding. J. Virol. 69 (1995): 1099-1106.
- [9] Farina, V. and Brown, J. D. Tamiflu: the supply problem. Angew. Chem. Int. Ed. 45 (2006): 7330-7334.
- [10] Kim, C. U.; Lew, W.; Williams, M. A.; Liu, H.; Zhang, L.; Swaminathan, S.; Bischofberger, N.; Chen, M. S.; Mendel, D. B.; Tai, C. Y.; Laver, W. G. and Stevens, R. C. Influenza neuraminidase inhibitors possessing a novel hydrophobic interaction in the enzyme active site: design, synthesis, and structural analysis of carbocyclic sialic acid analogues with potent anti-influenza activity. J. Am. Chem. Soc. 119 (1997): 681–690.
- [11] Subbarao, K. and Joseph, T. Scientific barriers to developing vaccines against avian influenza viruses. Nat. Rev. Immunol. 7 (2007): 267–278.

- [12] Shibasaki, M. and Kanai, M. Synthetic strategies for oseltamivir phosphate. Eur. J. Org. Chem. (2008): 1839–1850.
- [13] Oxford, J. S.; Bossuyt, S.; Balasingam, S.; Mann, A.; Novelli, P and Lambkin, R. (2003). Treatment of epidemic and pandemic influenza with neuraminidase and M2 proton channel inhibitors. Clin. Microbiol. Infect. 9 (2003): 1-14.
- [14] Colman, P. M.; Varghese, J. N. and Laver, W. G. Structure of the catalytic and antigenic sites in influenza virus neuraminidase. Nature 303 (1983): 41–44.
- [15] Varghese, J. N.; McKimm-Breschkin, J. L.; Caldwell, J. B.; Kortt, A. A. and Colman, P. M. The structure of the complex between influenza virus neuraminidase and sialic acid, the viral receptor. Proteins: Struct. Funct. Genet. 14 (1992): 327–332.
- [16] Itzstein, M. V.; Wu, W.-Y.; Kok, G. B.; Pegg, M. S.; Dyason, J. C.; Jin, B.; Phan, T. V.; Smythe, M. L.; White, H. F.; Oliver, S. W.; Colman, P. M.; Varghese, J. N.; Ryan, D. M.; Woods, J. M.; Bethell, R. C.; Hotham, V. J.; Cameron, J. M. and Penn, C. R. Rational design of potent sialidase-based inhibitors of influenza virus replication. Nature 363 (1993): 418–423.
- [17] Graul, A.; Leeson, P. A. and Castaner, J. Oseltamivir phosphate: anti-influenza, neuraminidase (sialidase) inhibitor. Drugs Future 24 (1999): 1189–1202.
- [18] Rohloff, J. C.; Kent, K. M.; Postich, M. J.; Becker, M. W.; Chapman, H. H.; Kelly, D. E.; Lew, W.; Louie, M. S.; McGee, L. R.; Prisbe, E. J.; Schultze, L. M.; Yu, R. H. and Zhang, L. Practical total synthesis of the anti-influenza drug GS-4101. J. Org. Chem. 63 (1998): 4545-4550.
- [19] Federspiel, M.; Fischer, R.; Henning, M.; Mair, H-J.; Oberhauser, T.; Rimmler, G.; Albiez, T.; Bruhin, J.; Estermann, H.; Gandert, C.; Gockel, V.; Gotzo, S.; Hoffmann, U.; Huber, G.; Janatsch, G.; Lauper, S.; Rockel-Stabler, O.; Trussardi, R. and Zwahlen, A. G. Industrial synthesis of the key precursor in the synthesis of the anti-influenza drug oseltamivir phosphate (Ro 64-0796/002, GS-4104-02): Ethyl(3R,4S,5S)-4,5-epoxy-3-(1-ethyl-propoxy)-cyclohex-1-ene-1-carboxylate. Org. Proc. Res. Dev. 3 (1999): 266-274.
- [20] McGowan, D. A. and Berchtold, G. A. (-)-Methyl cis-3-Hydroxy-4,5-oxycyclohex-1-enecarboxylate: stereospecific formation from and conversion to (-)-methyl

- shikimate; complex formation with bis(carbomethoxy)hydrazine. J. Org. Chem. 46 (1981): 2381-2383.
- [21] Kim, C. U.; Lew, W.; Williams, M. A.; Wu, H.; Zhang, L.; Chen, X.; Escarpe, P. A.; Mendel, D. B.; Laver, W. G. and Steven, R. C. Structure-activity relationship studies of novel carbocyclic influenza neuraminidase inhibitors. J. Med. Chem. 41 (1998): 2451-2460.
- [22] Karpf, M. and Trussardi, R. European Patent EP 1 059 283 A1, Dec 13, (2000).
- [23] Karpf, M. and Trussardi, R. New, Azide-Free Transformation of Epoxides into 1,2-Diamino Compounds: Synthesis of the Anti-Influenza Neuraminidase Inhibitor Oseltamivir Phosphate (Tamiflu). J. Org. Chem. 66 (2001): 2044-2051.
- [24] Harrington, P. J.; Brown, J. D.; Foderaro, T. and Hughes, R. C. Research and development of a second-generation process for oseltamivir phosphate, prodrug for a neuraminidase inhibitor. Org. Process Res. Dev. 8 (2004): 86-91.
- [25] Abrecht, S.; Karpf, M.; Trussardi, R. and Wirz, B. EP 1127872 A1, 2001, Chem. Abstr. 135 (2001): 195452.
- [26] Yeung, Y.-Y.; Hong, S. and Corey, E. J. A Short enantioselective pathway for the synthesis of the anti-influenza neuramidase inhibitor oseltamivir from 1,3-butadiene and acrylic acid. J. Am. Chem. Soc. 128 (2006): 6310-6311.
- [27] Mu, F.; Coffing, S. L.; Riese, D. J.; Geahlen, R. L.; Verdier-Pinard, P. Hamel, E.; Johnson, J. and Cushman, M. Design, Synthesis, and Biological Evaluation of a Series of Lavendustin A Analogues That Inhibit EGFR and Syk Tyrosine Kinases, as Well as Tubulin Polymerization. J. Med. Chem. 44 (2001): 441-452.
- [28] Knapp, S. and Levorse, A. T. Synthesis and reactions of iodo lactams. J. Org. Chem. 53(1988): 4006-4014.
- [29] Bromfield, K. M.; Grade, H.; Hagberg, D. P.; Olsson, T. and Kann, N. An iron carbonyl approach to the influenza neuraminidase inhibitor Oseltamivir. Chem. Commun. (2007): 3183-3185.

- [30] Kipassa, N. T.; Okamura, H.; Kina, K.; Hamada, T. and Iwagawa, T. Efficient short step synthesis of Corey's Tamiflu intermediate. Org. Lett. 10 (2008): 816-817.
- [31] Trost, B. M. and Zhang, T. A Concise Synthesis of (-)-Oseltamivir. Angew. Chem. Int. Ed. 47 (2008): 3759–3761.
- [32] Singer, S. P. and Sharpless, K. B. Synthesis of dl-gabaculine utilizing direct allylic amination as the key step. J. Org. Chem. 43 (1978): 1448-1455.
- [33] Danishefsky, S. and Hershenson, F. M. Regiospecific synthesis of isogabaculine. J. Org. Chem. 44 (1979): 1180-1181.
- [34] Trost, B. M. and Keinan, E. An approach to primary allylic amines via transition-metal-catalyzed reactions. Total synthesis of (±)-gabaculine. J. Org. Chem. 44 (1979): 3451-3457.
- [35] Bandara, B. M. R.; Birch, A. J. and Kelly, L. F. Superimposed lateral control of structure and reactivity exemplified by enantiospecific synthesis of (+)- and (-)-gabaculine. J. Org. Chem. 49 (1984): 2496-2498.
- [36] Frater, G.; Müller, U. and Schöpfer, U. Regioselective synthesis of (±)-gabaculine hydrochloride. Tetrahedron Lett. 25 (1984): 281-284.
- [37] Hiemstra, H.; Klaver, W. J. and Speckamp, W. N. Regioselective synthesis of (±)-gabaculine. Tetrahedron Lett. 27 (1986):1411-1414.
- [38] Flynn, D. L.; Zelle, R. E. and Grieco, P. A. A mild two-step method for the hydrolysis of lactams and secondary amides. J. Org. Chem. 48 (1983): 2424-2426.
- [39] Morris, G. M.; Huey, R.; Lindstrom, W.; Sanner, M. F.; Belew, R. K.; Goodsell, D. S. And Olson, A. J. AutoDock4 and AutoDockTools4: automated docking with selective receptor flexibility. J. Comput. Chem. 30 (2009): 2785–2791.
- [40] Cheng, L. S.; Amaro, R. E.; Xu, D.; Li, W. W.; Arzberger, P. W. and McCammon, A. J. Ensemble-based virtual screening reveals potential novel antiviral compounds for avian influenza neuraminidase. J. Med. Chem. 51 (2008): 3878–3894.
- [41] García-Sosa, A. T.; Sild, S. and Maran, U. Design of multi-binding-site inhibitors, ligand efficiency, and consensus screening of avian influenza H5N1 wild-type

- neuraminidase and of the oseltamivir-resistant h274y variant. J. Chem. Inf. Model. 48 (2008): 2074–2080.
- [42] Kalliokoski, T.; Salo, H. S.; Lahtela-Kakkonen, M. and Poso, A. The effect of ligand-based tautomer and protomer prediction on structure-based virtual screening. J. Chem. Inf. Model. 49 (2009): 2742–2748.
- [43] Durrant, J. D. and McCammon, J. A. Potential drug-like inhibitors of Group 1 influenza neuraminidase identified through computer-aided drug design. Comput. Biol. Chem. 34 (2010): 97–105.
- [44] Shendage, D. M.; Frohlich, R. and Haufe, G. Highly Efficient Stereoconservative Amidation and Deamidation of α -Amino Acids. Org. Lett. 6 (2004): 3675–3678.
- [45] Rabideau, P. W.; Wetzel, D. M.; Young, D. M. Metal-ammonia ring reduction of aromatic carboxylic acid esters. J. Org. Chem. 49 (1984): 1544–1549.
- [46] Hook, J. M. and Mander, L. N. Recent developments in the Birch reduction of aromatic compounds: applications to the synthesis of natural products. Nat. Prod. Rep. 3 (1986): 35–84.
- [47] Khan, A. T.; Parvin, T.; Gazia, S. and Choudhury, L. H. Bromodimethylsulfonium bromide mediated Michael addition of amines to electron deficient alkenes. Tetrahedron Lett. 48 (2007): 3805–3808.
- [48] Weeresakare, G. M.; Xua, Q. and Rainier, J. D. An anionic condensation and fragmentation approach to substituted 3-pyrrolines. Tetrahedron Lett. 43 (2002): 8913–8915.
- [49] Liu, Z. and Rainier, J. D. Ring-opening/ring-closing metathesis (rorcm) reactions of 7-azanorbornene derivatives: an entry into perhydroindolines. Org. Lett. 8 (2006): 459–462.
- [50] Frisch, M. J.; Trucks, G. W.; Schlegel, H. B.; Scuseria, G. E.; Robb, M. A.; Cheeseman, J. R.; Montgomery, Jr., J. A.; Vreven, T.; Kudin, K. N.; Burant, J. C.; Millam, J. M.; Iyengar, S. S.; Tomasi, J.; Barone, V.; Mennucci, B.; Cossi, M.; Scalmani, G.; Rega, N.; Petersson, G. A.; Nakatsuji, H.; Hada, M.; Ehara, M.; Toyota, K.; Fukuda, R.; Hasegawa, J.; Ishida, M.; Nakajima, T.; Honda, Y.; Kitao, O.; Nakai, H.; Klene, M.; Li, X.; Knox, J. E.; Hratchian, H. P.;

- Cross, J. B.; Bakken, V.; Adamo, C.; Jaramillo, J.; Gomperts, R.; Stratmann, R. E.; Yazyev, O.; Austin, A. J.; Cammi, R.; Pomelli, C.; Ochterski, J. W.; Ayala, P. Y.; Morokuma, K.; Voth, G. A.; Salvador, P.; Dannenberg, J. J.; Zakrzewski, V. G.; Dapprich, S.; Daniels, A. D.; Strain, M. C.; Farkas, O.; Malick, D. K.; Rabuck, A. D.; Raghavachari, K.; Foresman, J. B.; Ortiz, J. V.; Cui, Q.; Baboul, A. G.; Clifford, S.; Cioslowski, J.; Stefanov, B. B.; Liu, G.; Liashenko, A.; Piskorz, P.; Komaromi, I.; Martin, R. L.; Fox, D. J.; Keith, T.; Al-Laham, M. A.; Peng, C. Y.; Nanayakkara, A.; Challacombe, M.; Gill, P. M. W.; Johnson, B.; Chen, W.; Wong, M. W.; Gonzalez, C.; and Pople, J. A. Gaussian 03. Gaussian, Inc., Wallingford CT. 2004.
- [51] Russell, R. J.; Haire, L. F.; Stevens, D. J.; Collins, P. J.; Lin, Y. P.; Blackburn, G. M.; Hay, A. J.; Gamblin, S. J. and Skehel, J. J. The structure of H5N1 avian influenza neuraminidase suggests new opportunities for drug design. Nature 44 (2006): 45-49.
- [52] Ha, Y.; Stevens, D. J.; Skehel, J. J. and Wiley, D. C. X-ray structures of H5 avian and H9 swine influenza virus hemagglutinins bound to avian and human receptor analogs. Proc. Natl. Acad. Sci. USA 98 (2001): 11181-11186.
- [53] AutoDock tool. Available from: <http://autodock.scripps.edu/resources/adt/index.html> [2009, May 5].
- [54] Morris, G. M.; Huey, R.; Lindstrom, W.; Sanner, M. F.; Belew, R. K.; Goodsell, D. S. And Olson, A. J. AutoDock4 and AutoDockTools4: automated docking with selective receptor flexibility. J. Comput. Chem. 30 (2009): 2785–2791.
- [55] Sotriffer, C. A.; Winger, R. H.; Liedl, K. R.; Rode, B. M.; and Varga, J. M. Comparative docking studies on ligand binding to the multispecific antibodies IgE-La2 and IgE-Lb4. J. Comput. Aided. Mol. Des. 10 (1996): 305-320.
- [56] ChemBridge Screening Library [online]. Available from: <https://scifinder.cas.org/scifinder/view/scifinder/scifinderExplore.jsf> [2009, May 31].
- [57] Betschart, C.; Lerchner, A.; Machauer, R.; Rueeger, H.; Tintelnot-Blomley, M. and Veenstra, S. J. Preparation of macrocyclic lactones for treatment of β -amyloid related disease. PCT Int. appl.WO2006074950 (2006).

- [58] Edwards, L.; Isaac, M.; Johansson, M.; Kers, A.; Malmberg, J.; McLeod, D.; Mindis, A.; Staaf, K.; Slassi, A. and Stefanac, T. Preparation of heteropolycyclic compounds and their use as metabotropic glutamate receptor antagonists. U.S. Pat. Appl. publ. US 20050272779 A1 20051208 (2005) .
- [59] Frydman, B. and Ojeze, M. I. 1,4-Diaminobutanes From Furans: A New Synthetic Approach to Substituted Putrescines. Tetrahedron Lett. 39 (1998): 4765-4768.
- [60] Gourlay, B. S.; Molesworth, P. P.; Ryan, J. H. and Smith, J. A. A new and high yielding synthesis of unstable pyrroles via a modified Clauson-Kaas reaction. Tetrahedron Lett. 47 (2006): 799–801.
- [61] Edeleva, M. V.; Kirilyuk, I. A.; Zubenko, D. P.; Zhurko, I. F.; Marque, S. R. A.; Gignes, D.; Guillaneuf, Y.; Bagryanskaya, E. G. Kinetic study of H-atom transfer in imidazoline-, imidazolidine-, and pyrrolidine-based alkoxyamines: Consequences for nitroxide-mediated polymerization. J. Poly. Sci., Part A: Poly. Chem. 47 (2009): 6579-6595.
- [62] Sun, H.; Lin, Y. J.; Wu, Y. L. and Wu., Y. A Facile Access to Antiflu Agent Tamiflu/Oseltamivir. Synlett 2009, No. x, A–D.
- [63] Kamimura, A. and Nakano, T. Use of the Diels-Alder Adduct of Pyrrole in Organic Synthesis. Formal Racemic Synthesis of Tamiflu. J. Org. Chem. 75 (2010): 3133–3136.
- [64] Oh, S. H.; Kim, S. J.; Lee, S. J.; Choi, S. A.; Lee, Y. J.; Kim, H.; Lee, S. Method of preparation of aza-bicyclo[2.2.1] heptene derivative and oseltamivir intermediate. PCT Int. Appl. WO 2010074387 A1 20100701 (2010).
- [65] Cohen-Daniel, L.; Zakay-Ronesb, Z.; Resnick, I. B.; Shapira, M. Y.; Dorozhko, M.; Mador, N.; Greenbaum, E. and Wolf, D. G. Emergence of oseltamivir-resistant influenza A/H3N2 virus with altered hemagglutination pattern in a hematopoietic stem cell transplant recipient. J. Clin. Virol. 44 (2009): 138–140.



APPENDIX

ศูนย์วิทยทรัพยากร
จุฬาลงกรณ์มหาวิทยาลัย

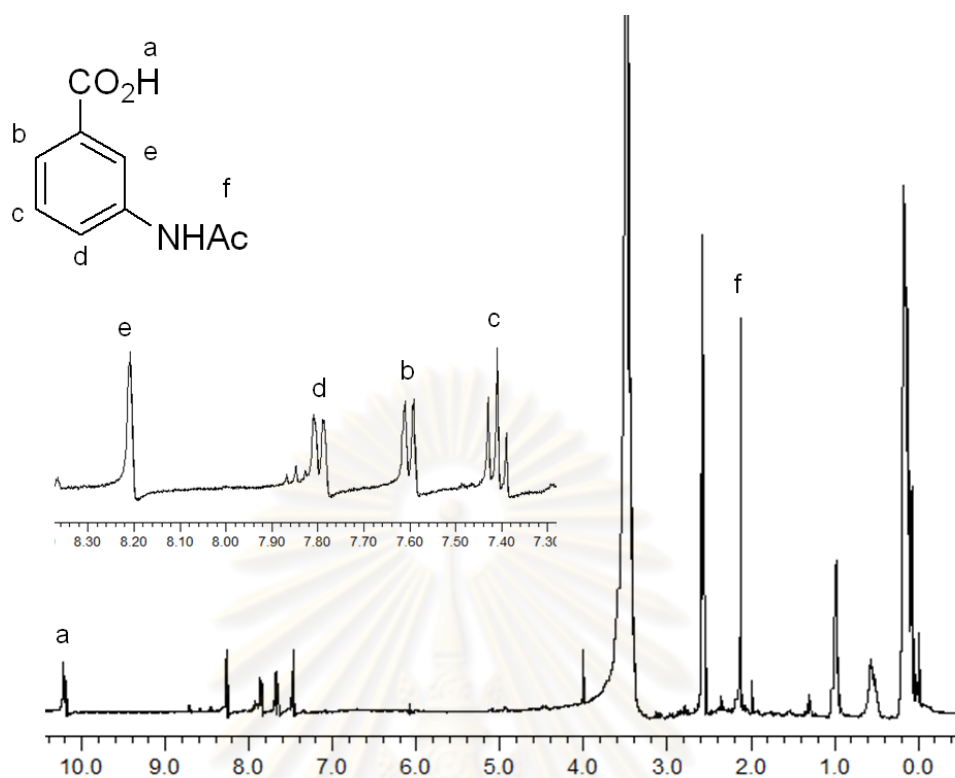


Figure A.1 $^1\text{H-NMR}$ (DMSO) Spectrum of 3-acetamidobenzoic acid **78** in a mixture

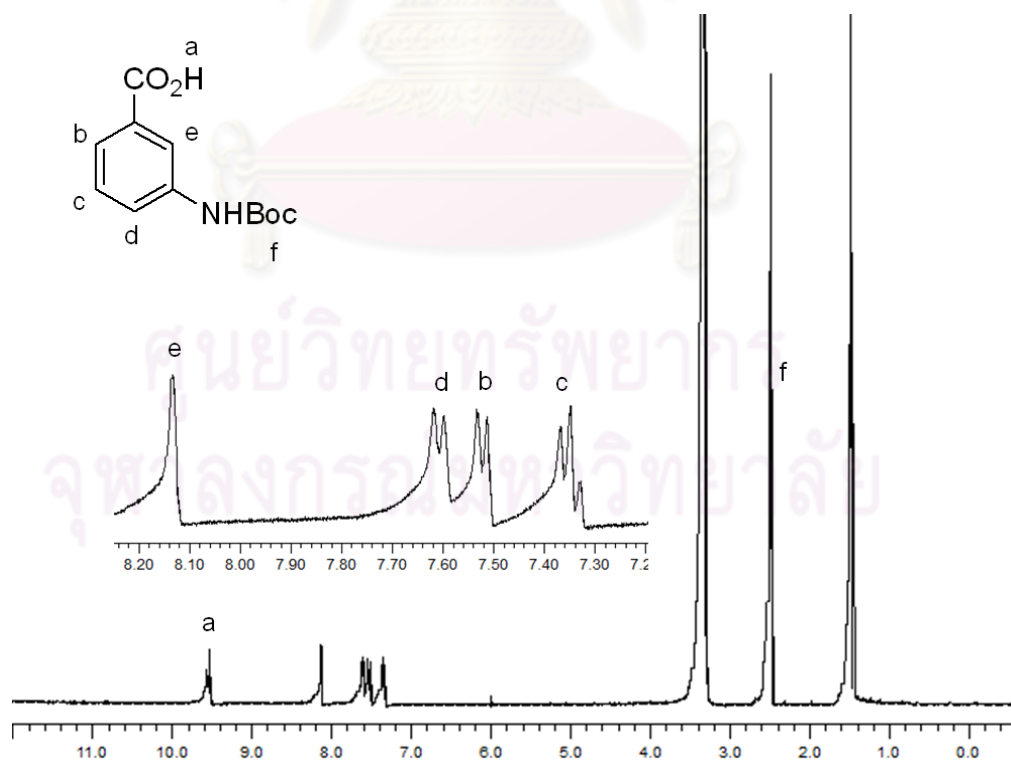


Figure A.2 $^1\text{H-NMR}$ (DMSO) Spectrum of 3-[(*tert*-butoxycarbonyl)amino]benzoic acid **72**

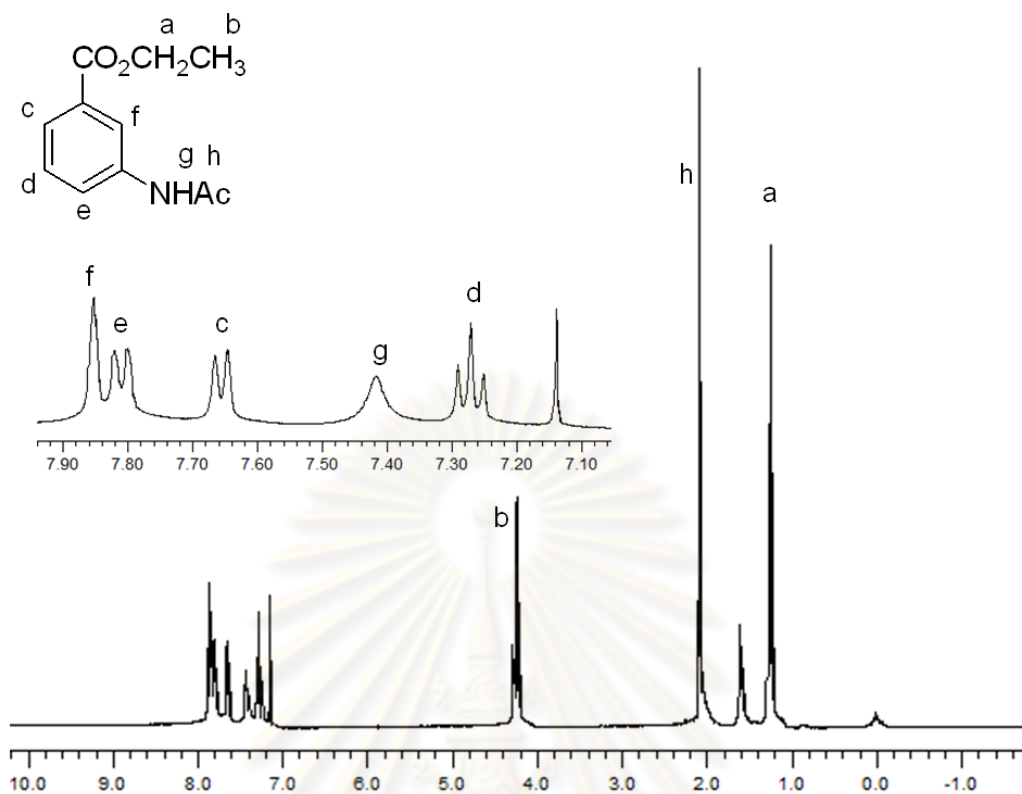


Figure A.3 $^1\text{H-NMR}$ (CDCl_3) Spectrum of ethyl-3-acetamidobenzoate **79**

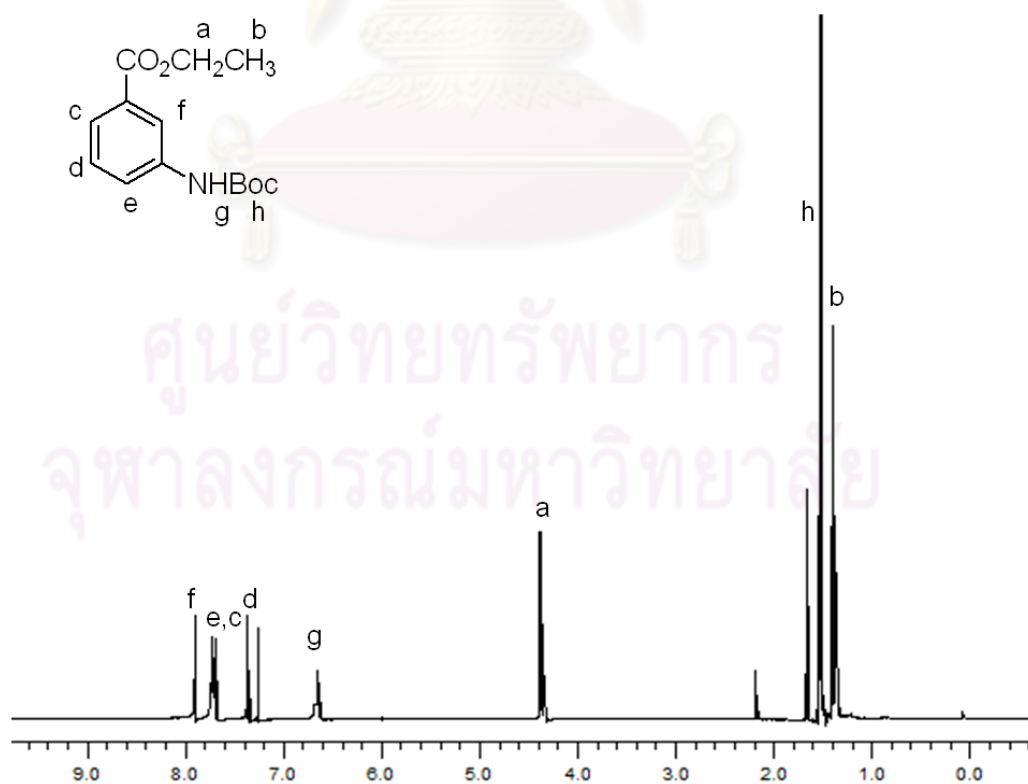


Figure A.4 $^1\text{H-NMR}$ (CDCl_3) Spectrum of ethyl-3-(*tert*-butoxycarbonyl)benzoate **73**

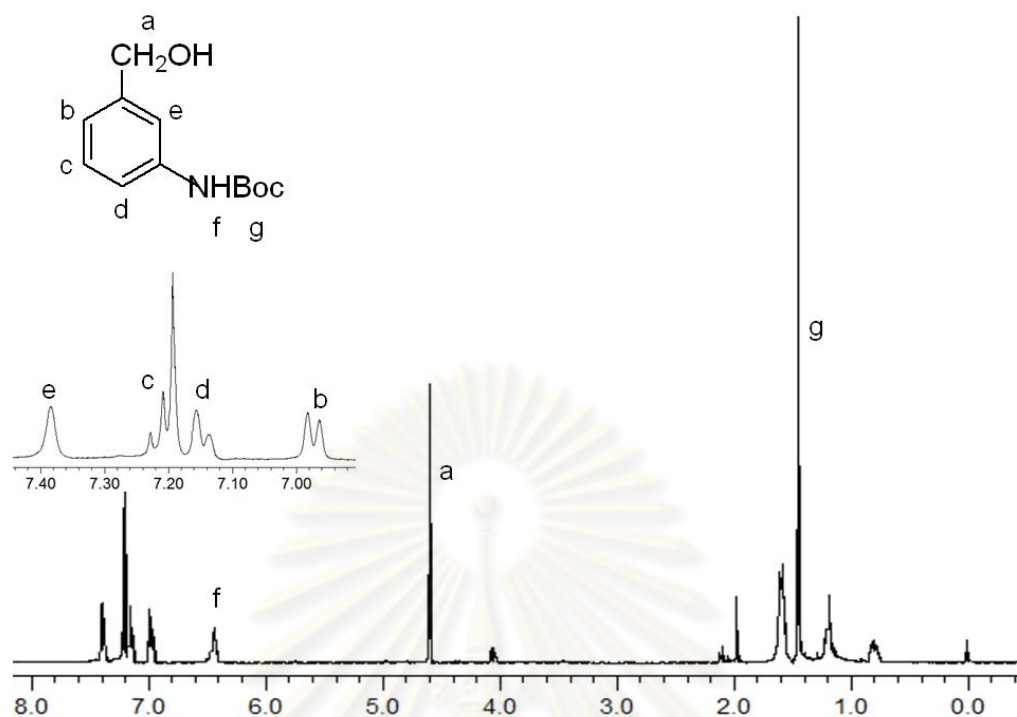


Figure A.5 $^1\text{H-NMR}$ (CDCl_3) Spectrum of *tert*-Butyl[3-(hydroxymethyl)phenyl] carbamate **89** in a mixture

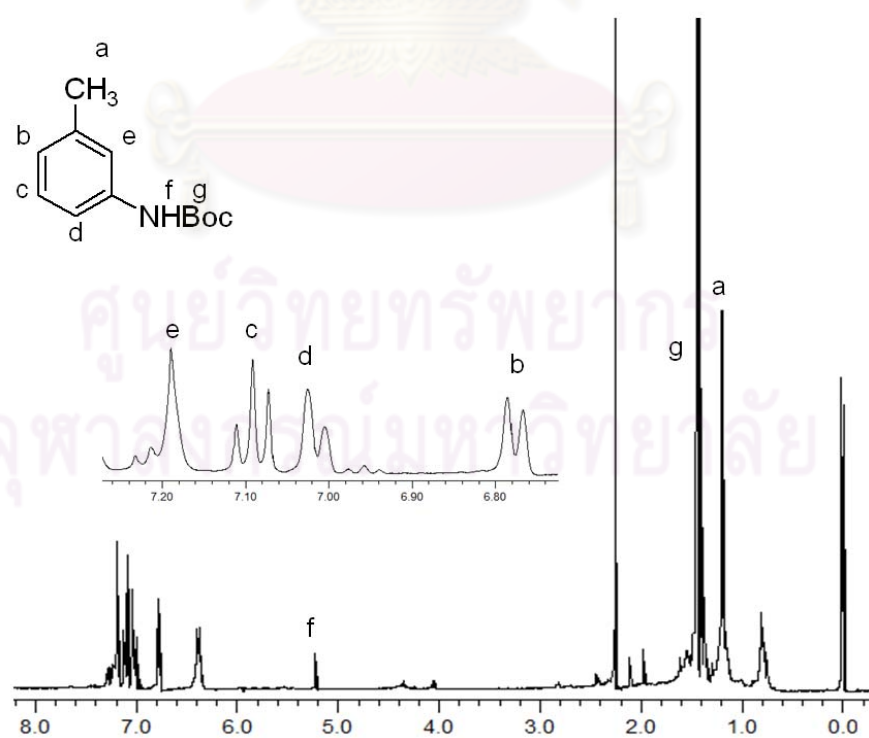


Figure A.6 $^1\text{H-NMR}$ (CDCl_3) Spectrum of *N*-(*tert*-butoxycarbonyl)-*m*-toluidine **90** in a mixture

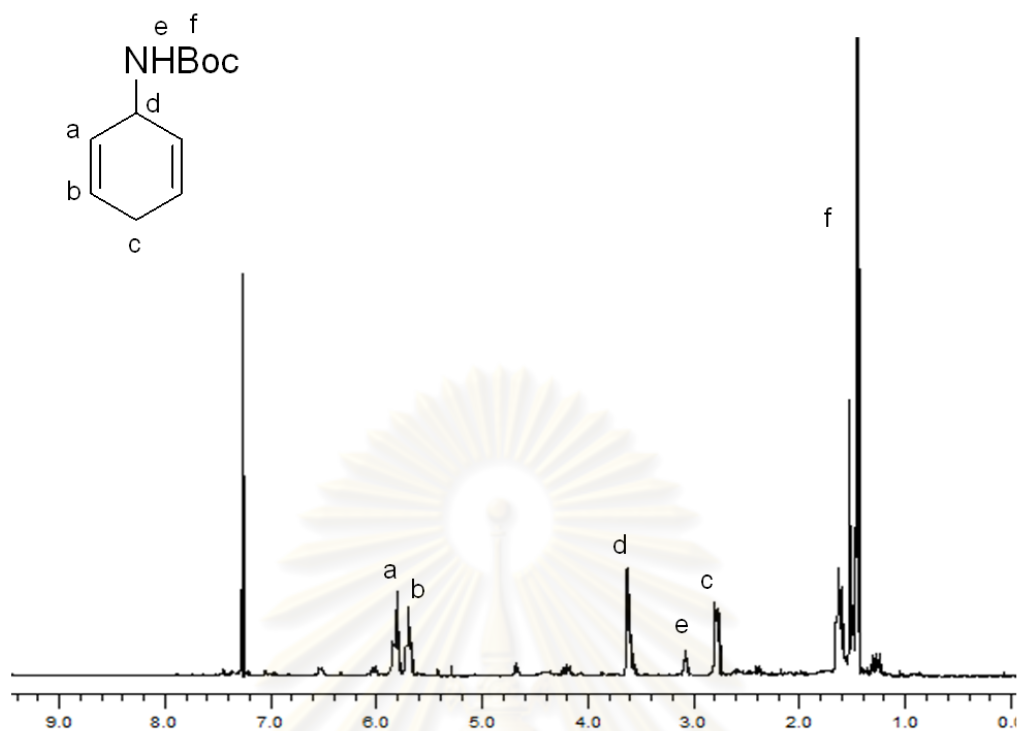


Figure A.7 ¹H-NMR (CDCl₃) Spectrum of *tert*-butyl cyclohexa-2,5-dienylcarbamate **80**

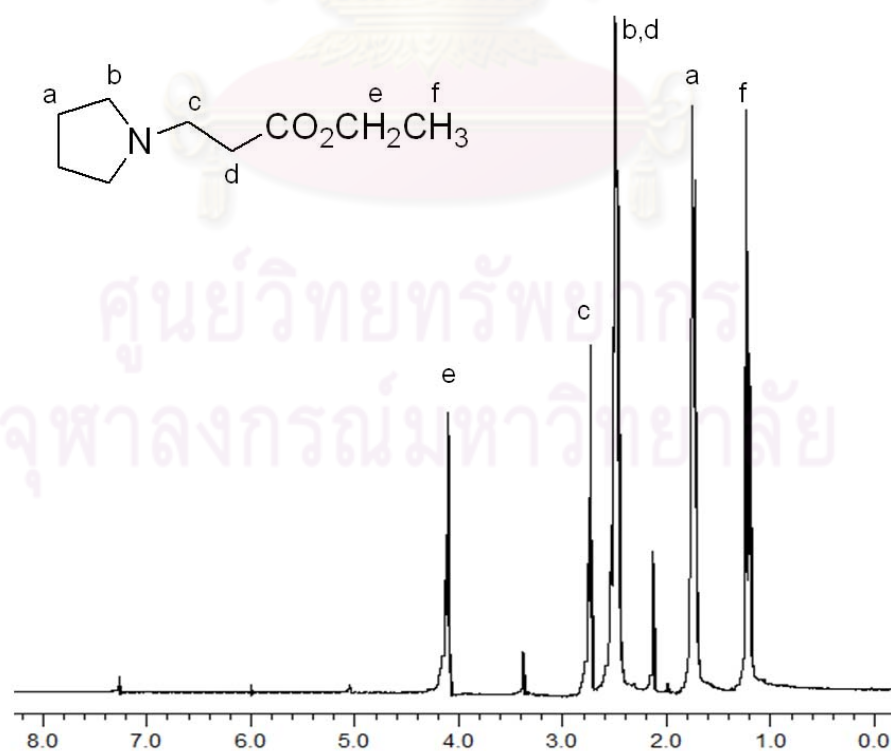


Figure A.8 ¹H-NMR (CDCl₃) Spectrum of ethyl-2-(*N*-pyrrolidiny)propanoate **81**

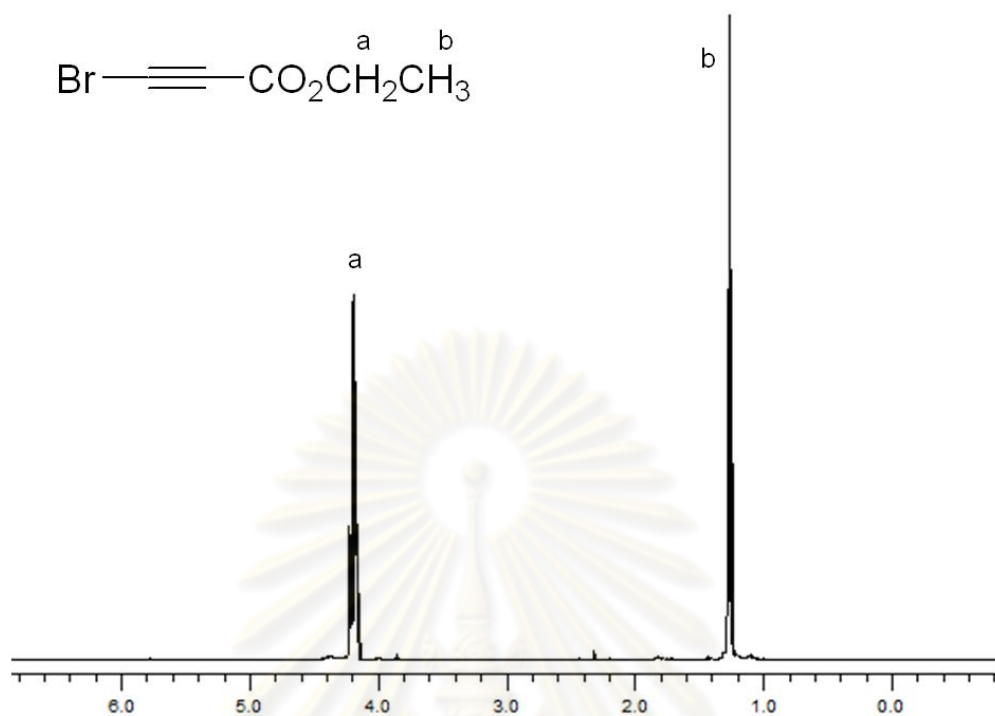


Figure A.9 ¹H-NMR (CDCl₃) Spectrum of ethyl 3-bromopropionate **82**

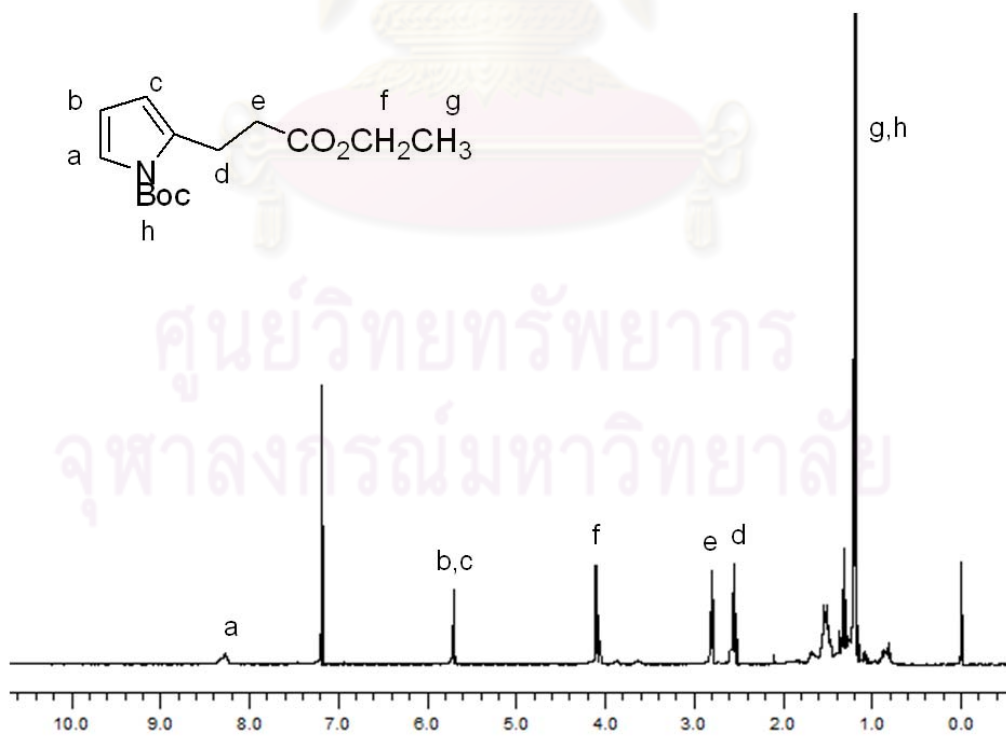


Figure A.10 ¹H-NMR (CDCl₃) Spectrum of ethyl-2-(*N*-*tert*-butoxycarbonyl)pyrrolyl propanoate **83**

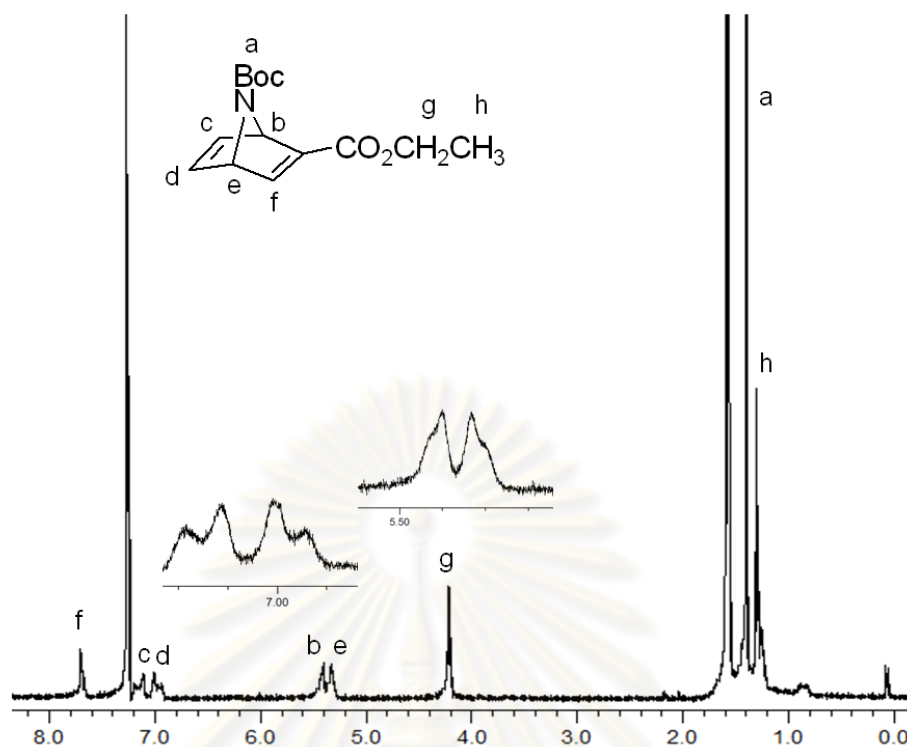


Figure A.11 $^1\text{H-NMR}$ (CDCl_3) Spectrum of 7-Azabicyclo[2.2.1]hepta-2,5-diene-2,7-dicarboxylic acid, 7-(1,1-dimethylethyl) 2-ethyl ester **85**

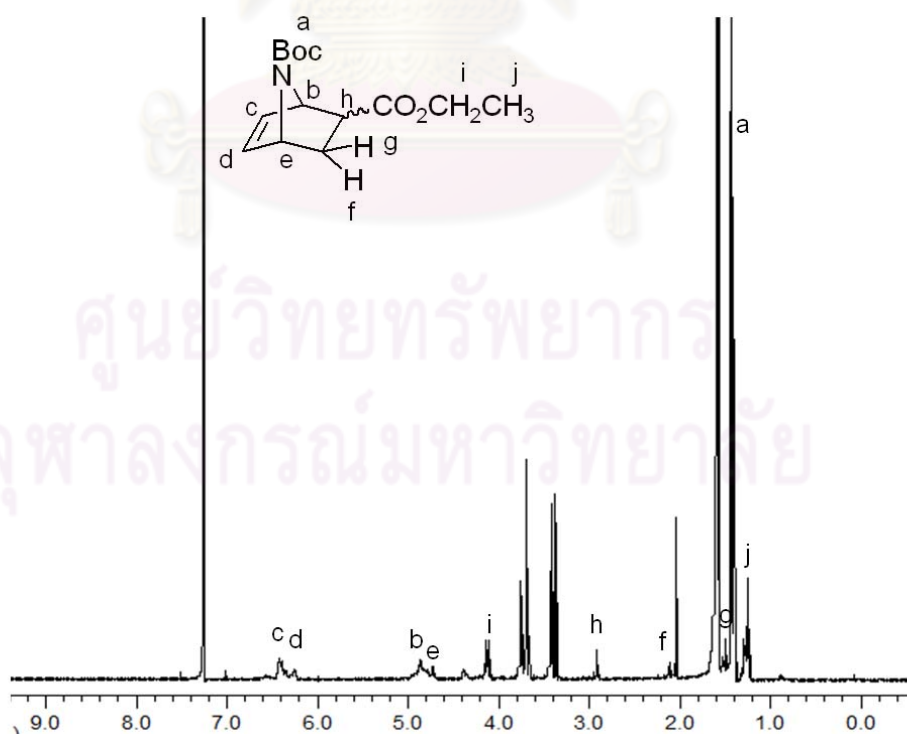


Figure A.12 $^1\text{H-NMR}$ (CDCl_3) Spectrum of 7-Azabicyclo[2.2.1]hept-5-ene-2,7-dicarboxylic acid, 7-(1,1-dimethylethyl) 2-ethyl ester **86**

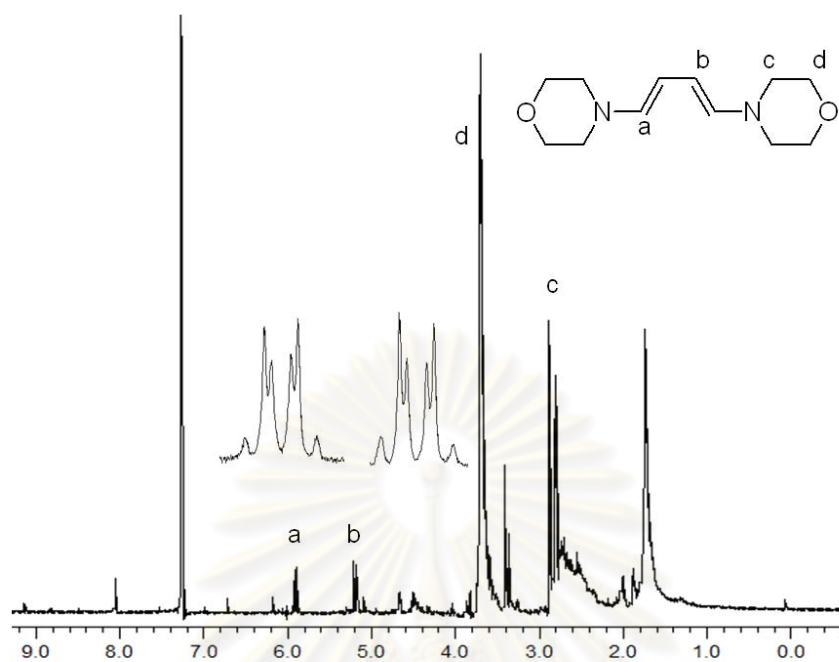


Figure A.13 $^1\text{H-NMR}$ (CDCl_3) Spectrum of 1,4(*N*-morpholinyl)-butadiene **97**

ศูนย์วิทยทรัพยากร
จุฬาลงกรณ์มหาวิทยาลัย

Table A.1 Docking results of the lowest energy rank (2HU4)

Cpds	Frequency	MeanE (kcal/mol)	RMSD (Å)	$E_{\text{vdw+Hb+dsol}}$ (kcal/mol)	E_{elec} (kcal/mol)
m1	24	-7.03	1.11267	-5.91	-2.85
m2	60	-7.28	0.4643	-4.99	-3.57
m3	13	-7.43	2.86336	-6.79	-2.32
m4	1	-7.39	4.97655	-5.91	-2.57
m5	23	-6.87	2.1109	-5.51	-1.94
m6	137	-8.11	0.43129	-6.01	-3.77
m7	51	-7.40	1.25978	-5.25	-4.07
m8	27	-5.99	5.37424	-5.82	-2.65
m9	152	-8.09	3.48967	-5.5	-4.19
m10	284	-7.56	1.00574	-5.28	-5.41
m11	125	-8.14	0.91113	-5.33	-4.55
m12	219	-8.17	0.90465	-5.31	-6.07
m13	191	-7.86	3.56309	-5.03	-4.60
m14	169	-6.70	0.65237	-5.10	-4.65
m15	159	-8.23	3.36001	-4.94	-4.29
m16	215	-8.63	0.47503	-5.82	-5.61
m17	166	-8.17	3.45278	-5.32	-4.20
m18	274	-7.78	0.85397	-4.97	-5.49
m19	78	-7.82	0.8781	-4.77	-5.46
m20	214	-8.04	0.57147	-5.11	-6.26
m21	87	-7.67	1.61494	-4.81	-5.39
m22	144	-7.13	0.50942	-4.97	-5.00
m23	134	-8.81	1.22913	-4.66	-6.08
m24	232	-9.01	0.47039	-5.48	-6.09
m25	120	-7.26	2.42321	-4.85	-3.14
m26	105	-7.45	0.8157	-5.00	-3.71
m27	94	-6.33	2.20515	-5.42	-3.16
m28	94	-6.99	0.96323	-5.40	-3.89
m29	403	-7.26	0.57575	-3.72	-4.02
m30	459	-7.82	0.86572	-4.24	-3.85
m31	31	-7.27	2.0116	-4.96	-3.43
m32	173	-7.01	0.44426	-5.21	-3.67
m33	25	-6.32	1.3106	-4.94	-3.73
m34	80	-6.53	0.69611	-5.17	-4.09
osel	79	-8.46	0.25032	-6.6	-4.24

Table A.2 Docking results of the highest frequency rank (2HU4)

Cpds	Cluster rank	Frequency	MeanE (kcal/mol)	RMSD (Å)	E _{vdw+Hb+dsol} (kcal/mol)	E _{elec} (kcal/mol)
m1	4	64	-5.66	4.57827	-4.87	-2.77
m2	1	60	-7.28	0.4643	-4.99	-3.57
m3	2	73	-7.25	2.17496	-4.00	-1.76
m4	30	43	-4.02	8.24091	-4.15	-1.23
m5	2	40	-6.51	1.95384	-5.04	-2.97
m6	1	137	-8.11	0.43129	-6.01	-3.77
m7	2	67	-6.46	4.62624	-5.23	-2.87
m8	2	76	-6.66	0.96748	-4.45	-3.74
m9	1	152	-8.09	3.48967	-5.50	-4.19
m10	1	284	-7.56	1.00574	-5.28	-5.41
m11	2	154	-8.16	3.24733	-5.19	-4.83
m12	1	219	-8.17	0.90465	-5.31	-6.07
m13	1	191	-7.86	3.56309	-5.03	-4.60
m14	1	169	-6.70	0.65237	-5.10	-4.65
m15	1	159	-8.23	3.36001	-4.94	-4.29
m16	1	215	-8.63	0.47503	-5.82	-5.61
m17	1	166	-8.17	3.45278	-5.32	-4.20
m18	1	274	-7.78	0.85397	-4.97	-5.49
m19	9	90	-5.74	4.50159	-4.59	-3.16
m20	1	214	-8.04	0.57147	-5.11	-6.26
m21	3	110	-7.39	3.0342	-2.76	-4.22
m22	1	144	-7.13	0.50942	-4.97	-5.00
m23	2	160	-8.18	3.09436	-5.13	-4.92
m24	1	232	-9.01	0.47039	-5.48	-6.09
m25	1	120	-7.26	2.42321	-4.85	-3.14
m26	1	105	-7.45	0.8157	-5.00	-3.71
m27	1	94	-6.33	2.20515	-5.42	-3.16
m28	1	94	-6.99	0.96323	-5.40	-3.89
m29	1	403	-7.26	0.57575	-3.72	-4.02
m30	1	459	-7.82	0.86572	-4.24	-3.85
m31	2	76	-6.52	4.77535	-4.74	-3.12
m32	1	173	-7.01	0.44426	-5.21	-3.67
m33	3	67	-6.24	4.19948	-4.95	-3.31
m34	1	80	-6.53	0.69611	-5.17	-4.09
osel	1	79	-8.46	0.25032	-6.60	-4.24

Table A.3 Docking results of the lowest energy rank (1JSN)

Cpds	Frequency	MeanE (kcal/mol)	RMSD (Å)	$E_{vdw+Hb+dsol}$ (kcal/mol)	E_{elec} (kcal/mol)
m1	64	-5.00	12.95498	-4.65	-1.84
m2	4	-5.19	12.32604	-5.66	-0.55
m3	7	-5.83	13.81086	-6.32	-0.32
m4	3	-5.55	12.67678	-6.04	-0.54
m5	3	-5.28	16.22065	-5.72	-1.54
m6	19	-4.95	11.67016	-4.86	-1.64
m7	1	-5.78	5.18726	-4.90	-1.63
m8	10	-5.84	12.72396	-6.67	-0.34
m9	23	-7.02	17.95826	-3.32	-5.55
m10	22	-5.50	20.9455	-3.46	-4.88
m11	26	-6.30	20.28338	-3.96	-3.52
m12	26	-5.81	20.55831	-4.16	-4.53
m13	24	-6.29	18.78536	-3.37	-4.70
m14	20	-5.89	20.49044	-4.14	-5.25
m15	21	-6.30	20.36761	-3.06	-4.32
m16	36	-6.15	20.48961	-3.62	-4.73
m17	33	-6.87	17.77643	-3.68	-5.22
m18	15	-5.97	21.31803	-3.77	-4.32
m19	35	-5.79	20.16213	-4.26	-3.25
m20	28	-5.67	20.57788	-3.73	-4.59
m21	26	-6.17	18.04617	-3.51	-5.00
m22	28	-6.28	20.80254	-3.51	-5.47
m23	16	-5.75	21.07028	-3.71	-3.89
m24	25	-6.34	20.25772	-3.41	-5.00
m25	51	-5.76	12.03208	-5.16	-1.87
m26	1	-6.55	17.79827	-4.63	-2.34
m27	8	-4.58	21.73278	-3.91	-2.61
m28	20	-5.41	20.23895	-4.22	-2.84
m29	53	-6.21	11.56051	-5.30	-1.75
m30	74	-5.21	12.15539	-5.28	-1.93
m31	5	-5.32	18.17989	-4.48	-2.58
m32	2	-5.36	18.08242	-4.57	-2.77
m33	312	-6.09	17.34387	-3.67	-2.94
m34	41	-5.48	21.97762	-3.22	-2.53
sial	5	-5.67	6.87222	-4.53	-1.21

Table A.4 Docking results of the highest frequency rank (2HU4)

Cpds	Cluster rank	Frequency	MeanE (kcal/mol)	RMSD (Å)	$E_{vdw+Hb+dsol}$ (kcal/mol)	E_{elec} (kcal/mol)
m1	2	231	-5.11	9.34893	-3.10	-3.10
m2	8	110	-4.75	10.48134	-3.53	-2.31
m3	3	194	-4.96	8.82882	-2.93	-3.19
m4	6	135	-4.22	10.0445	-3.29	-2.52
m5	8	99	-5.41	9.50045	-2.77	-3.20
m6	10	88	-4.36	9.87154	-2.77	-2.72
m7	11	115	-4.80	9.5398	-2.93	-2.83
m8	8	100	-4.58	10.12167	-2.55	-3.01
m9	3	250	-5.83	9.19454	-2.86	-4.36
m10	4	119	-4.80	9.00662	-3.10	-4.74
m11	3	280	-5.37	9.35324	-2.99	-3.64
m12	3	328	-5.20	9.11858	-3.39	-4.51
m13	11	115	-4.86	11.61649	-1.90	-4.39
m14	5	100	-4.56	10.19655	-3.63	-3.86
m15	12	146	-5.69	11.35456	-2.33	-3.71
m16	2	186	-4.77	9.12939	-3.68	-3.80
m17	4	250	-5.79	9.3005	-3.04	-4.07
m18	9	142	-5.19	9.01915	-2.91	-4.79
m19	4	135	-4.72	8.75632	-2.59	-3.92
m20	3	225	-5.04	9.09711	-3.53	-4.61
m21	9	131	-5.17	9.34184	-3.31	-4.04
m22	6	148	-4.82	10.3351	-3.61	-3.90
m23	3	236	-5.43	8.74109	-2.93	-4.02
m24	5	165	-5.13	9.11962	-3.82	-3.78
m25	4	237	-5.45	9.53196	-2.89	-2.79
m26	8	104	-4.82	10.59266	-3.25	-2.71
m27	3	257	-5.00	9.08182	-3.12	-3.07
m28	12	145	-4.42	9.41595	-2.79	-3.01
m29	2	102	-5.79	8.88469	-3.56	-2.96
m30	1	74	-5.21	12.15539	-5.28	-1.93
m31	2	134	-5.08	10.41879	-3.52	-3.16
m32	16	88	-3.99	9.29982	-3.04	-2.92
m33	1	312	-6.09	17.34387	-3.67	-2.94
m34	2	201	-5.24	17.46108	-3.31	-2.13
sial	3	22	-5.52	10.21871	-4.01	-1.51

VITAE

Name: Ms. Naruwan Pattarapongdilok

Date of Birth: May 6th, 1985

Address: 42/33 Yarnviroch Rd., T. Kaokhang, A. Muang, Chanthaburi, 22000

Email: olinpoo@gmail.com

Education:	YEAR	INSTITUTION	DEGREE
	2004	Benjamarachutit Chanthaburi High School	
	2008	Chulalongkorn Univ.	B.Sc. (Chemistry)
	2010	Chulalongkorn Univ.	M.Sc. (Chemistry)

Scholarship and Awards:

- 2008-2010 -Full scholarship from National Center of Excellence for Petroleum, Petrochemicals and Advanced Materials (NCE-PPAM)
- 2008 -Research grant from Chemistry-CU Research Experience Undergraduates (Chem-CU REU)
- Award for best manner and best activist honored by department of chemistry, faculty of science, Chulalongkorn University for academic year 2007
- 2007 -Award for best manner of department of chemistry honored by faculty of science, Chulalongkorn University for academic year 2006
- 2006 -First runner-up of The Inventer and Innovator Project
- 2004 -Full scholarship from Human resource development in science project

Presentation in Conferences:

- Pattarapongdilok N., Sritana-anant Y. and Sompornpisut P., *In-silico designed neuraminidase inhibitors based on derivatives of oseltamivir*, Pure and Applied Chemistry International Conference (PACCON) 2010, 21st-23rd January 2010, Sunee Grand Hotel and Convention Center, Ubon Ratchathani.
- Pattarapongdilok N., Sritana-anant Y. and Sompornpisut P., *Molecular docking of in-silico designed neuraminidase inhibitors based on an alternative route of oseltamivir synthesis*, The 5th Mathematics and Physical Sciences Graduate Congress, 7th-9th December 2009, Faculty of Science, Chulalongkorn University, Bangkok.
- Niyomdecha M., Pattarapongdilok N., Sritana-anant Y., Vilaivan T., *Application of Mitsunobu reaction in the introduction of amino substituent of Oseltamivir phosphate*, Organic synthesis research unit mini-symposium 2009, 12nd February 2009, Faculty of Science, Chulalongkorn University, Bangkok.